Validation of on-line nanoparticle surface area measurements using induced current techniques

Johannes Rex

DIVISION OF ERGONOMICS AND AEROSOL TECHNOLOGY | DEPARTMENT OF DESIGN SCIENCES
FACULTY OF ENGINEERING LTH | LUND UNIVERSITY
2022

MASTER THESIS

Validation of on-line nanoparticle surface area measurements using induced current techniques

Johannes Rex

LUND
UNIVERSITY

Validation of on-line nanoparticle surface area measurement using induced current techniques

Published by
Department of Design Sciences
Faculty of Engineering LTH, Lund University
P.O. Box 118, SE-221 00 Lund, Sweden

Subject: Aerosol Technology (MAMM05)
Division: Ergonomics and Aerosol Technology
Supervisor: Vilhelm Malmborg
Examiner: Axel Eriksson

Abstract

Soot is formed during incomplete combustion and has known adverse health effects as well as contributes to global warming. Soot particles are not spheres, but rather agglomerates of smaller primary soot particles. Specific surface area (SSA) and lung-deposited surface area (LDSA) are important metrics related to the toxicity of aerosols. To determine SSA the standard method is to employ gas adsorption and Brunauer-Emmett-Teller (BET) analysis, which requires large particle samples (~100 mg). Therefore, a simpler way to measure SSA is sought after. The aim of this thesis was to investigate such a method, which allows on-line surface area measurement, and validate against BET for different aerosol particles.

The Partector 2 instrument charges an aerosol by unipolar diffusion charging and measures an induced current in a Faraday cage. The number of electrical charges given to an aerosol particle is proportional to its surface area. The Partector 2 was used to measure total surface area and LDSA of combustion soot particles, engineered carbon blacks, and polystyrene latex (PSL) spheres. The aerosols were also measured after passing through a thermodenuder to remove volatile compounds. To determine SSA the mass of the aerosol was measured in two different ways, the equivalent carbon black (eBC) concentration by optical absorption, and by particle size distributions with the application of effective particle densities. The Partector 2 surface area and LDSA measurements were additionally validated by PSL spheres.

A proportionality between the surface area measured by the Partector 2 and that determined from the size distribution of spherical particles was found (R^2 = .997, n = 6), but with a considerable scaling factor. For the LDSA a proportionality was also found (R^2 = .993, n = 6) but with an even larger scaling factor. When using the surface area from the Partector 2 and the effective density to determine the mass, a reasonable agreement (±30%) was found when validating the SSA by BET analysis. This means that the Partector 2 instrument has the potential to be a good tool for on-line measurement and could favorably be used for health-related measurements, for example at a workplace. Because of the uncertainty found in this thesis, caution must be taken when using the Partector 2 results even in environments where particles can be assumed to have mainly spherical shapes, and especially so if particles have combustion origin. It could also be concluded that the SSA of the soot particles increased after the volatile compounds on them were removed after passing through a thermodenuder.

Keywords: specific surface area, soot, carbon black, nanoparticles, lung-deposited surface area, induced current

Sammanfattning

Sot bildas vid ofullständig förbränning och har kända negativa hälsoeffekter såväl som att det bidrar till den globala uppvärmningen. Sotpartiklar är inte sfäriska, utan består utav agglomerat av mindre primärpartiklar. Specifik ytarea och lung-deponerad ytarea är viktiga hälsorelaterade mått på aerosoler av nanopartiklar. Standardmetoden för att bestämma den specifika ytarean består av gasadsorption och Brunauer-Emmett-Teller (BET) analys, vilket kräver stora mängder partiklar (ca 0.1 g). Det finns därför ett behov av en enklare och smidigare metod att bestämma den specifika ytarean. Målet med detta examensarbete är att utvärdera en sådan metod, som möjliggör ”on-line” ytarea mätningar, och validera den mot BET för ett flertal olika partiklar.

Partectorinstrumentet laddar en aerosol med unipolär diffusion och mäter den inducerade strömmen från en Faraday bur. Antalet laddningar som en partikel får är proportionell mot dess ytarea. Partectorn användes för att mäta den totala ytarean och lung-deponerade ytarean på sotpartiklar, carbon blacks och polystyrene latex (PSL) sfärer. Aerosolerna mättes också efter de fick passera igenom en termodenuder för att avlägsna volatila ämnen. För att kunna bestämma den specifika ytarean bestämdes massan av aerosolerna på två olika sätt, den ekvivalenta black carbon (eBC) koncentrationen genom optisk absorption och genom partiklarnas storleksfördelning tillsammans med partiklarnas effektiva densitet. Partectorns ytarea och lung-deponerade ytarea mätningar validerades även mot sfäriska kalibreringspartiklar.

En linjär korrelation fanns mellan ytarean mätt av Partectorn och den bestämd av storleksfördelningen (R^2 = .997, n = 6), men trendlinjen avvek kraftigt från en lutningskoefficient på 1. För den lungdeponerade ytarean fanns också en proportionalitet (R^2 = .993, n = 6) och med en ännu större avvikning. Specifik ytarea mätt av Partectorn, där massan bestämdes av storleksfördelningen tillsammans med den effektiva densiteten, visade en rimlig överenskommelse när den jämfördes mot BET analysen. Det visades dock att värdena inte är exakta, utan ger en rimlig uppskattning med en felmarginal (upp mot ±30 %). Detta betyder att Partectorn har god potential för on-linemätningar av ytarean i hälsorelaterade mätningar, till exempel vid olika arbetsplatser. Men, på grund av avvikelsen mot referensmätningarna som upptäcktes i detta examensarbetet bör försiktighet tas vid användning av mätvärdena. En slutsats kunde också dras att den specifika ytarean hos partiklarna ökade något efter att de passerat igenom en termodenuder.

Nyckelord: specifik ytarea, sot, carbon black, nanopartiklar, lung-deponerad ytarea, inducerad ström

Populärvetenskaplig sammanfattning

Utvärdering av ytarea mätning på nanopartiklar med inducerad ström

Luftföroreningar påskyndar den globala uppvärmingen och orsakar hälsoproblem som leder till att cirka sju miljoner människor dör i förtid varje år. Mycket forskning har gjorts på mikrometerstora partiklar, men forskning kvarstår framför allt på mindre partiklar i nano-storlek.

På grund av att nanopartiklar är väldigt små så har de mycket yta i förhållande till sin vikt. Studier har visat att ytarean av inhalerade partiklar bidrar mer till de negativa hälsoeffekterna i lungorna än vikten av partiklarna. Ett mått som är relevant för att jämföra denna ytarean är den specifika ytarean, som är ytarean per viktenhet (m^2/g). Ett annat relevant mått är den lungdeponerade ytarean som beskriver hur mycket ytarea som fastnar i lungorna vid inandning. Eftersom ytarean av små partiklar är betydelsefull för hälsan så finns det ett behov av en enkel metod att fastställa den. Den dominerande metoden för att fastställa den specifika ytarean kräver i dagsläget en stor mängd uppsamlade partiklar och tar lång tid. I detta arbete utvärderades en metod där man kan mäta ytarean och den lungdeponerade ytarean direkt i luften. I metoden laddas partiklarna med elektroner och passerar igenom instrumentet som mäter en inducerad ström som de laddade partiklarna ger upphov till. Detta sker i realtid och kan implementeras i en handhållen apparat som kan användas både inomhus och utomhus, till exempel direkt vid en arbetsplats. Syftet med arbetet var att utvärdera hur noggrann metoden är för att mäta ytarean av olika typer av nanopartiklar, så att framtida forskning vet om de kan förlita sig på den.

I detta examensarbete mättes ytarean, den specifika ytarean och den lungdeponerade ytarean på sotpartiklar som bildats vid ofullständig förbränning och på tillverkade ”carbon blacks” (kimrök) som till exempel används som ett fyllnadsmaterial i däck, plast och i färg. I arbetet kunde det påvisas att ytarean och den lungdeponerade ytarean kunde mätas med den beskrivna metod men att det fortfarande krävs kalibrering av instrumentet för att få ett pålitligt mätvärde.

Acknowledgments

I would like to thank all the people at the division of Aerosol Technology who helped me in any way during my thesis, and everyone else who contributes to the nice atmosphere at the division.

I would especially like to thank my supervisor Vilhelm Malmborg for his support and patience during my project. Thank you for all you have taught me in the field of aerosols, your knowledge and insight have been invaluable.

I would also like to thank Sara Blomberg for teaching me how to do BET analysis, and for helping me in the BET lab.

Lund, June 2022

Johannes Rex

Table of contents

List of acronyms and abbreviations

BC	black carbon
BET	Brunauer-Emmett-Teller
CB	carbon black
CPC	condensation particle counter
d_p	particle diameter
DF_{AL}	ICRP alveolar deposition fraction
DMA	differential mobility analyzer
EAD	electrical aerosol detector
eBC	equivalent black carbon
EC	elementary carbon
ENP	engineered nanoparticle
GMD	geometric mean diameter
GSD	geometric standard deviation
HEPA	high efficiency particulate arresting
ICRP	International Commission on Radiological Protection
k_{SA}	surface area correction constant
LDSA	lung-deposited surface area
NP	nanoparticle
OC	organic carbon
OC/TC	organic carbon to total carbon ratio
PSL	polystyrene latex
ρ_{eff}	effective density
SA	surface area
SA_{NM}	nucleation mode surface area
SA^c	corrected surface area
SMPS	scanning mobility particle sizer
SSA	specific surface area
SSA_{BET}	specific surface area from BET
SSA_{eBC}	specific surface area derived from Partector 2 and microAeth
SSA^c_{eBC}	specific surface area derived from corrected Partector 2 and microAeth
SSA_{eff}	specific surface area from Partector 2 and SMPS with effective density

SSA^{c}_{eff}	specific surface area from corrected Partector 2 and SMPS with effective density
TD	thermodenuder
TEM	transmission electron microscopy
UT	untreated (bypass)
WHO	World Health Organisation

1 Introduction

1.1 Background

Aerosols are a suspension of solid and/or liquid particles in a gas, such as air (Hinds, 1999). Black carbon (BC) soot particles are common solid particles found in the air that are formed during incomplete combustion. These particles are emitted into the air from many different sources such as burning of fossil fuels, biofuels, and biomass - both by anthropogenic activities and natural phenomena such as wildfires (World Health Organization, 2021).

Soot particles are not spheres, but rather agglomerates of smaller primary soot particles. Figure 1.1 illustrates soot and nanoparticles formed in diesel exhaust (Mariqc, 2007). In the figure it is also illustrated that the agglomerates are usually coated with organic compounds and inorganics. Smaller nucleation mode particles are also illustrated. Nucleation mode particles derive from nucleated particles of 1-3 nm that grow to nucleation mode particles (>3 nm)(Guo et al., 2020).

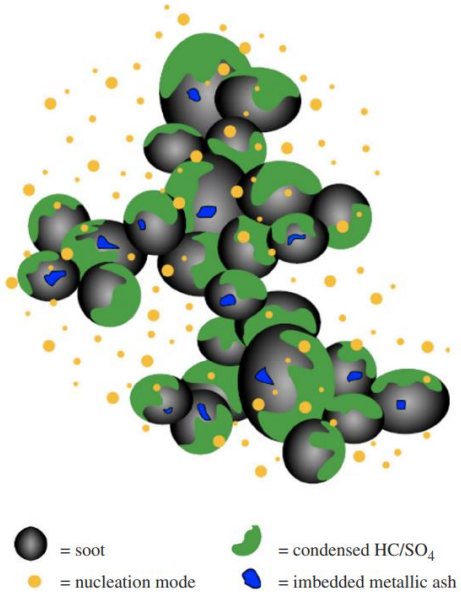

Figure 1.1 Illustration of a diesel soot particle. Printed with Permission (Mariqc, 2007).

In this thesis combustion related soot particles were investigated as well as carbon blacks, which are a form of engineered nanoparticles (ENP). Carbon blacks are used as a filler in tires and other rubber products, as well as in paints, plastics, and printing inks (Ceresana, 2022).

According to the World Health Organisation (WHO) air pollution is one of the biggest environmental threats to human health and is estimated to cause 7 million premature deaths annually (World Health Organisation, 2022). The negative effects of exposure and inhalation of combustion related particles have been common knowledge for a long time. Known effects of continued exposure include cancer, lung disease, and heart disease (Kumfer & Kennedy, 1991). It is debated exactly what causes the negative health effects, however evidence that chronic exposures to carbon black and diesel soot cause tumor formation because of its carbon core (Kumfer & Kennedy, 1991). Although WHO are aware of the scientific evidence of the adverse health effects of black carbon, they have yet to set specific recommendations like the ones set for $PM_{2.5}$ and PM_{10} i.e., particulate matter of sizes below 2.5 µm and 10 µm respectively (World Health Organization, 2021). Soot particles contain black carbon also contributes to global warming due to their light-absorbing properties (Dalirian, 2018).

Toxicological studies on rats and mice have shown that surface area of aerosol nanoparticles is one of the most important metrics related to the pulmonary toxicity (Schmid & Stoeger, 2016). Since nanoparticles have a much larger surface area to mass ratio than bigger particles, this suggests that they are more toxic compared to larger particles. To add to this theory studies have also shown that when comparing nanoparticles of the size of 20 nm to the size of 250 nm, the inflammatory response when using the same mass was much larger for the smaller particle, however, when instead correcting for the surface area the inflammatory response was linear when exposed to both sizes (Oberdöster et al., 2005). Soot and carbon black are solid agglomerated particles with high surface area to mass ratio. Exposures occur primarily as a result of emissions from human activities. Characterizing soot surface area is therefore of particular interest.

Since the specific surface area (SSA, m^2/g) of nanoparticle aerosols is an important metric, a simple and easy way to measure it is sought after. The standard procedure to determine surface area is by quantifying gas adsorption on particle surfaces and is based on Brunauer-Emmett-Teller (BET) theory that requires a large quantity of particle mass, 50-100 mg, which is often not possible to collect when dealing with nanoparticle aerosols. Another common method is the analysis of transmission electron microscopy (TEM) images and knowledge of the size of primary soot particles (Bourrous et al. 2018). TEM analysis is an "off-line" technique in that it first requires sampling of particles on small grids followed by analysis in a microscope. A third method is to charge the aerosol and measure the induced current from particles travelling in an air flow. The aerosol is charged by diffusion charging, which is the process of ions randomly colliding with particles, giving the particle the charge of the ion. The number of charges attached to a particle increases with surface area available for interaction. Such methods can be employed directly at the aerosol source, with direct and thus time-resolved information on nanoparticle surface area.

In this master thesis, as the title suggests, the method to determine the surface area of nanoparticles by charging and measuring induced currents is of interest. The method is based on pulsed unipolar diffusion charging of the aerosol by a corona charger after which the aerosol passes through a faraday cage where the charge of the particles is measured without the need of collecting the particles (Fierz et al., 2014). This allows for on-line (real time) measurement of surface area. This method is potentially very useful

because of the simplicity and mobility of the instrument, allowing for easy use in both indoor and outdoor environments. The instrument used in this thesis is the Partector 2.

Complementary to physical metrics like surface area concentration or particle number, other metrics more related to the effects on the human body have been developed, such as lung-deposited surface area (LDSA). The purpose of the LDSA metric is to measure particle surface area that will end up in the lungs. An empirical link between the electrical signal acquired from unipolar diffusion charging (EAD signal) and LDSA has been found and therefore some electrical instruments like the Partector 2 can measure LDSA. In this thesis LDSA will also be measured by the Partector 2 and validated.

1.2 Aim

The aim of this master thesis project is to validate the Partector 2 instrument and measurement of specific surface area on combustion related soot particles and engineered carbon black nanoparticles.

1.3 Research questions

- How accurate are measurements of aerosol surface area and LDSA by induced currents with the Partector 2 instrument for non-spherical agglomerate black carbon-containing and spherical particles?
- What are the effects on surface area measurements when volatile material is coating the particles?

2 Theory

2.1 Nanoparticles

Nanoparticles are usually defined as particles with around 1 nm to 100 nm diameter and sometimes up to a few hundred nm. In this master thesis particles in the size range of 10 nm to 350 nm in diameter were investigated and for simplicity these particles were denoted as nanoparticles.

2.2 Lung-deposited surface area

Complementary to physical metrics like surface area concentration or particle number, other metrics more related to the effects on the human body have been developed, such as lung-deposited surface area (LDSA). The purpose of the LDSA metric is to measure particles (and the resulting area) that will end up in the lungs which essentially means

$$LDSA = surface\ area\ \cdot deposition\ probability. \tag{2.1}$$

The deposition probability for this metric is defined as the deposition probability in the alveolar region. The deposition fraction for the alveolar region provided by the ICRP is

$$\mathrm{DF_{AL}}(d_p) = \frac{0.0155}{\mathrm{d_p}}\left(\exp\left(-0.416\left(\ln \mathrm{d_p} + 2.84\right)^2\right) + 19.11\exp\left(-0.482\left(lnd_p - 1.362\right)^2\right)\right) \tag{2.2}$$

where d_p is the particle diameter in µm (Hinds, 1999). The deposition fraction for the alveolar region relevant to the scope of this thesis is shown in Figure 2.1.

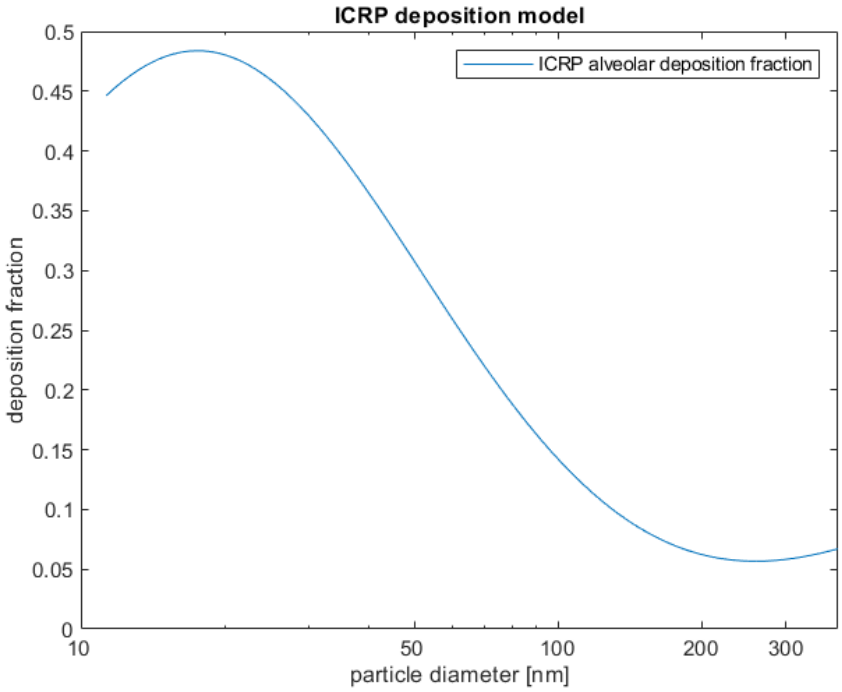

Figure 2.1 ICRP deposition model for the alveolar region.

LDSA is considered a toxicologically relevant metric (Kuuluvainen et al., 2016). Wilson et al. coined the term LDSA when they discovered that the surface area estimated to be deposited in the respiratory system (ICRP model) correlated well with the signal from an electrical aerosol detector (EAD) (2007). Because of this, LDSA can be estimated after unipolar diffusion charging which allows measuring instruments like the Naneos Partector 2 to measure LDSA in real time.

2.3 Partector theory

In this section theory relevant to the Partector 2 will be introduced. A short explanation of unipolar diffusion charging and aerosol measurements by induced currents are followed by a brief explanation of how the Partector 2 functions.

2.3.1 **Unipolar diffusion charging**

Diffusion charging is the process of ions randomly colliding with particles, giving the particle the charge of the ion. Unipolar charging means the charging is realized with ions of only one polarity. The ions are usually created by a corona charger. An approximate expression for the number of charges $n(t)$ that a particle of diameter d_p acquires by diffusion charging during a time t is given by

$$n(t) = \frac{d_p kT}{2K_E e^2}\, ln\left[1 + \frac{\pi K_E d_p \bar{c}_i e^2 N_i t}{2kT}\right] \tag{2.1}$$

where $K_E = \frac{1}{4\pi\epsilon_0}$, $\bar{c}_i$ is the mean thermal speed of ions, N_i is the ion density, and t is the time spent in the charger (Hinds, 1999).
This means that a unipolar diffusion charger charges an aerosol in such a way that the particles will have an average charge $\bar{q}$ that is proportional to the diameter. This relationship has been empirically found to be proportional to $\bar{q} \sim d^x$, where x is dependent of the $N_i t$ product. The charging level is also to a lesser degree affected by morphology, ion properties, particle dielectric constant, gas pressure, and temperature (Baron et al., 2011).

The number of charges attached to a particle increases with surface area available for interaction. Non-spherical particles such as soot agglomerates have a higher surface area than a sphere of the same diameter. Therefore, agglomerates have a higher charge attachment with similar electric mobility (Wilson et al., 2007).

2.3.2 **Aerosol measurement by induced currents**

Aerosol measurement by induced currents is a method of sizing aerosols by measuring an induced current. Similar to many diffusion charging instruments the aerosol is charged by a unipolar charger. The key difference however, is that instead of measuring the current arising from deposition of charged particles I_D on an electrometer, the induced current I_I is measured as the charged aerosol passes through a Faraday cage. As a charged particle passes through the Faraday cage that by definition is grounded, an image charge proportional to the space charge but with the opposite sign $Q' = -c \cdot Q$ must be on the cage, where c is a geometric correction factor. The total current measured is

$$I = I_D + I_I = I_D - c \cdot \dot{Q} \quad (2.2)$$

where Q̇ is rate of change of the space charge. The aerosol flows through the faraday cage and the deposited current is negligible in comparison to the induced current (Fierz et al. 2014). Since the induced current is dependent on a change in the space charge of the aerosol, the unipolar charger works in controlled pulses. This method is considered "on-line" since the measurement can be done in real time.

With the method of aerosol measurement with induced currents comes some limitations. When using a positive unipolar charger, particles with a pre-existing charge cannot be neglected. This is because if a particle is already positively charged, a too high signal will be registered, and for a negatively charged particle the signal will be lower than expected. Hence neutral particles are ideal for this method.

2.3.3 **Naneos Partector 2**

The Partector 2 is a handheld instrument that uses aerosol measurement by induced currents to measure multiple metrics of an aerosol on-line. The instrument functions largely as described in the previous section but with a dual detection stage. This means that the Partector 2 uses two faraday cages, where the first one measures the total charge and the second one a reduced signal after an electrostatic precipitator selectively removes small particles, allowing for an estimation of the particle diameter.

In this thesis the surface area of the particles is especially of interest. The Partector 2 calculates an approximate surface area concentration in the following way,

$$S = N \cdot \pi \cdot d^2 \cdot e^{2ln^2\sigma} \quad (2.3)$$

where N is the particle number concentration, d is the particle diameter, and σ is the geometrical standard deviation (GSD). The reason this is considered an approximation is that assumptions must be made and because there is error propagation in the calculation.

To be able to do this calculation, the particle number, the particle diameter, and the GSD must first be determined. An assumption is made that the aerosol is a polydisperse lognormal distributed aerosol with a certain GSD. The Partector 2 is calibrated for lognormal particle size distributions with a GSD of 1.9, which according to the manufacturer is a reasonable

assumption for many environments (Partector 2 Operation Manual, 2022). The particle diameter is approximated by the stage ratio which is the ratio between the second and the first electrometer signal (EM2/EM1). The particle number is then calculated using the approximated particle diameter,

$$N = c \cdot EM1 \cdot d^{-1.1} \tag{2.4}$$

where c is a constant, and EM1 is the electrometer attached to the first faraday cage. The surface area is then calculated using Equation 2.3.

The Partector 2 also measures LDSA concentration. The sizes range for particles where the Partector 2 accurately can measure LDSA is 20 nm – 350 nm because this is where the correlation of the measured charge and the deposition probability correlate well, according to the manufacturer (Lung-deposited surface area, 2021).

2.3.4 **Naneos Partector TEM**

The Partector TEM, similarly to the Partector 2, is a handheld instrument that uses aerosol measurement by induced currents to measure an aerosol. This version of the Partector is only equipped with one electrometer attached to a faraday cage and can therefore not estimate a particle diameter. Therefore, the only metric measured by the Partector TEM is LDSA concentration. The Partector TEM is also equipped with a TEM grid sampler that allows for direct deposition on the grid after being measured by the non-destructive method.

2.4 Scanning mobility particle sizer

A scanning mobility particle sizer (SMPS) consists of a differential mobility analyzer (DMA) that takes in a polydisperse aerosol and selects a monodisperse aerosol, and a condensation particle counter (CPC) that counts the particles.

The DMA consists of a cylinder with a negatively charged rod in the middle to create an electrical field. A laminar flow of particle free air flows in the sheath between the exterior and the rod. The sample particles are neutralized to a known charge distribution (Fuchs equilibrium charge distribution) by a radioactive source before entering the cylinder. The particle stream is then injected in one end of the cylinder at the outside of

the sheath flow. The positively charged particles will move in the electrical field towards the middle at a rate that depends on their electrical mobility. Particles of a certain mobility will then exit through a slit at the other end of the cylinder while the rest exit with the air exhaust flow. By scanning the central rod voltage, a particle size distribution is built up.

The CPC grows particles by condensing a liquid (often butanol) on to them, and then measures the scattered laser signal from the droplets. The increased size allows measuring particles as small as 4 nm in diameter.

2.5 Aethalometer

An Aethalometer was used to determine the soot mass concentration of the aerosols. An aethalometer is an instrument that analyzes the optical properties of an aerosol by continuously depositing particles on a filter and measuring the change in the transmission of light. The microAeth MA300 operates with 5 LEDs with different wavelengths. Only the wavelength 880 nm is relevant to this thesis since at this wavelength the measurement is interpreted as the concentration of equivalent black carbon (eBC) (microAeth Operating Manual, 2018). eBC is often used synonymously to black carbon but is a more correct term for the mass concentration acquired from filter-based optical absorption methods (Petzold et al., 2013).

2.6 Effective density

Soot particles are not perfect spheres but are agglomerates formed by smaller, almost spherical, primary particles. Since the size of particles in aerosols are commonly measured by the mobility diameter yielded by an SMPS, there is a need for a way of calculating the mass of the particles from the mobility diameter.

A common definition, and the definition used in this thesis, of effective density (ρ_{eff}) is the fraction of measured particle mass to the particle volume calculated assuming the particles are spheres with the mobility diameter (DeCarlo et al., 2004).

In this thesis, the power laws of the effective densities for Aquadag and Fullerene soot determined by Gysel et al. (2011) were used to calculate an alternative soot mass to the eBC mass determined by the Aethalometer. These effective densities as well as an average of the two, used as an estimation for the other soot, are illustrated in Figure 2.2.

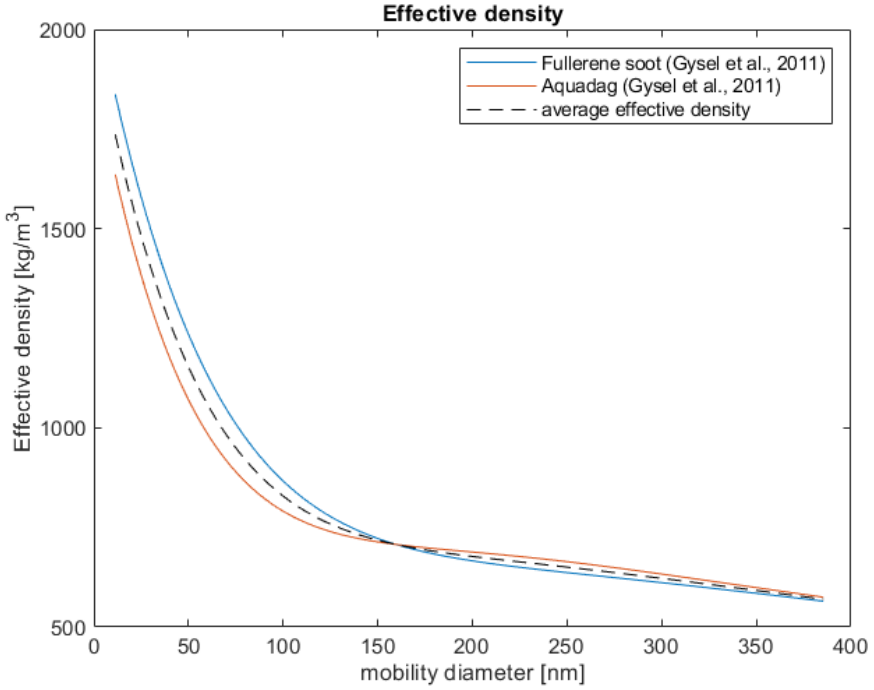

Figure 2.2 Effective density as a function of the mobility diameter for Fullerene soot, Aquadag, and an average of the two effective densities. Effective densities found by Gysel et al. (2011).

2.7 Brunauer-Emmett-Teller theory

Brunauer-Emmett-Teller (BET) theory is a commonly used method to measure surface area and is a widely accepted standard. Surface area measurement using BET theory involves exposing the sample to an inert adsorbate gas (typically nitrogen gas) in controlled increments and measuring the change in pressure and temperature. After every increment of adsorbent introduced, the pressure is allowed to equilibrate, and the amount adsorbed is calculated. If a monolayer was to be achieved this would give a very good measurement of the sample surface area, however in reality does not happen. The BET theory instead takes into account multilayer

adsorption as well. The graph acquired when adding adsorbent in small increments (and a desorption graph for when the gas is removed) is used to determine the amount of gas needed to form a monolayer from which the surface area can be calculated. An illustrative figure of the process is shown in Figure 2.3 (Micromeritics).

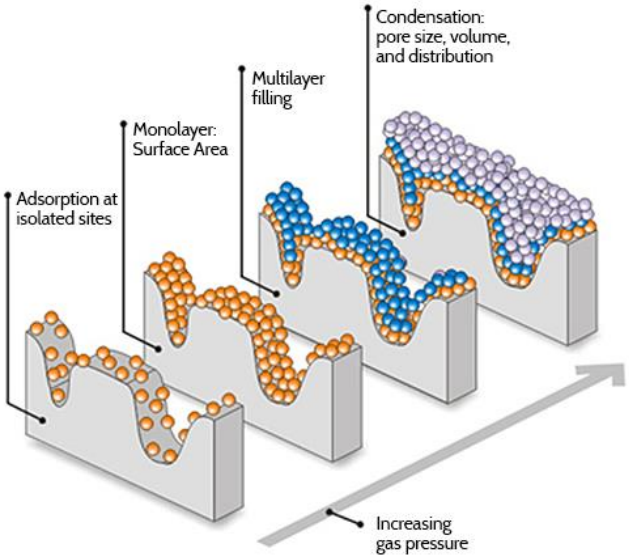

Figure 2.3 Illustration of mono- and multilayer adsorption during BET surface area analysis. Figure reproduced from Micromeritics with permission (Micromeritics).

BET requires large amounts, on the order of 100 mg, for the surface area analysis. However, it is not always possible to collect enough nanoparticles for the measurement due to the small amount of material one can obtain from the air. For studies of nanoparticle surface area, BET therefore often has limited use or is simply not an option.

3 Method

3.1 Aerosol lab set-up

The main lab set-up is shown in Figure 3.1. In the following subsection each part of the set-up is described in greater detail as well as the reference measurements performed.

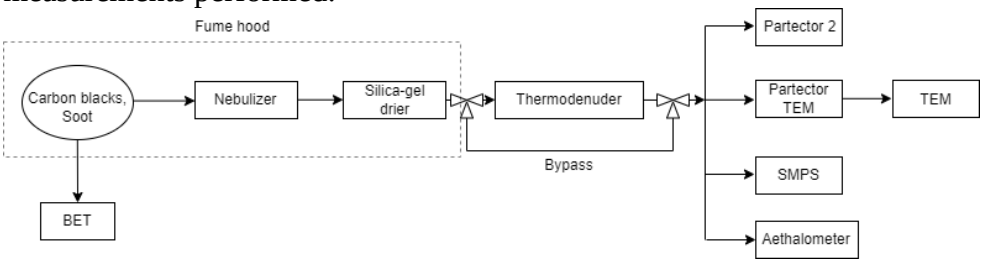

Figure 3.1 Schematic of the lab set-up in the Aerosol lab.

3.1.1 **Aerosol generation**

The aerosols used in this master thesis were generated using a nebulizer. The carbon black powders were first weighed (0.01 mg accuracy scale) then solved in deionized water (produced with reverse osmosis and capacitive deionization) at a concentration of 0.1 g/L. The mixture was put in an ultrasonic bath for 15 minutes to dissociate the soot powder. The bottle with the soot solution was then screwed into the nebulizer where it was put under 1 bar overpressure. The solution was then nebulized. The compressed air was first cleaned from volatile gas compounds and particles by two filters, an activated carbon filter and a high efficiency particulate arresting (HEPA) filter, before entering the lab set-up. The aerosol was then led through a tube where the concentration of the aerosol could be adjusted with a valve needle connected to the cleaned compressed air. Then the aerosol was led through a silica-gel drier before going to the thermodenuder or the bypass line.

The generation of the aerosols as well as the exhausts from the SMPS and the Aethalometer took place in a fume hood. To minimize electrostatic losses, all the tubing that the generated aerosols passed through were conductive Tygon tubing. The fume hood with the nebulizer is shown in Figure 3.2.

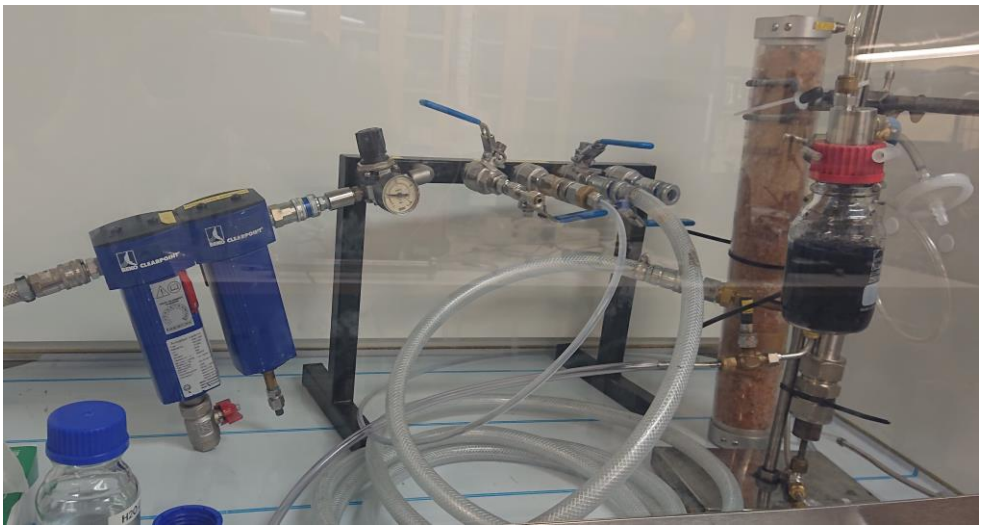

Figure 3.2 Picture of the fume hood containing the compressed air filters, nebulizer, silica-gel dryer, and a soot solved in water being nebulized.

Four types of carbon blacks (Fullerene soot, Regal carbon black R400, Aquadag, Printex 90) and soot from two gas-burners (Ethylene-air and miniCAST propane-air soot) were used in the study. Nebulizing the deionized water resulted in a nucleation mode of particles. This background from nebulizing deionized water was measured separately and subtracted from the soot aerosols (explained in section 4.2.4). Well-defined polystyrene latex (PSL) spheres with diameters of 220 nm, 269 nm, and 350 nm (density 1.05 g/m^3) were also measured for reference.

The thermodenuder and the instruments, Partector 2, Partector TEM, microAeth and the SMPS system are shown during measurement in Figure 3.3.

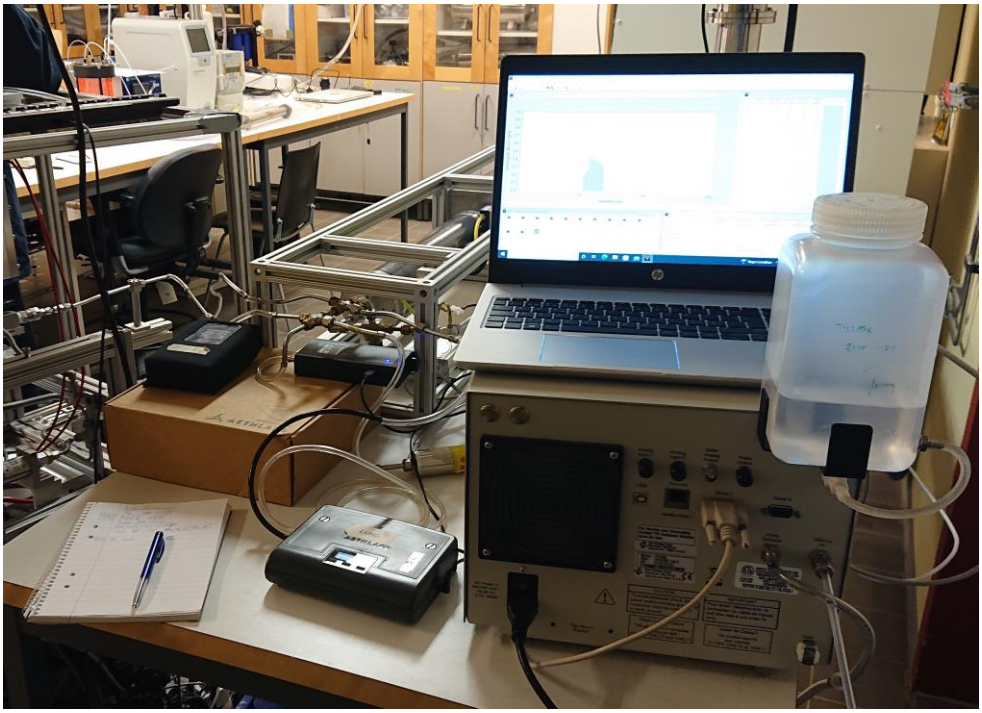

Figure 3.3 Partector 2, Partector TEM, microAeth MA300, and SMPS connected to the thermodenuder.

3.1.2 **Bypass and Thermodenuder**

The aerosol was either lead to the instruments directly through a bypass line, or through the thermodenuder to first remove volatile compounds. The thermodenuder was used to remove any pre-existing coating on the particles. A temperature of 250 ˚C was used since at this temperature elemental carbon (EC) such as soot particles are non-volatile whilst volatile material such as organic carbon (OC) on the particles is efficiently evaporated and will be removed from the gas phase in the active charcoal denuder. All aerosols were measured both passing through the thermodenuder and untreated by passing through the bypass line instead.

3.1.3 **Scanning mobility particle sizer**

An SMPS system was used to determine the size distribution of the aerosols. The DMA is a TSI model 3081 and the CPC is a TSI model 3775 that uses butanol for condensing on the particles.

The SMPS system was set to a low flow rate, 0.300 L/min, with a sheath flow of 6 L/min. Diffusion Loss Correction and Multiple Charge Correction was turned on. Each scan sequence was 120 s, with a 20 s flush time in between. The scan produced size bins between 11.3 nm and 385.4 nm with 99 total bins. Every aerosol was measured for 5 whole scans.

3.1.3.1 SMPS size distribution and log-normal fit

The average of the 5 SMPS scans were taken after which the SMPS size distribution data was fit to a log-normal two-term gaussian model, allowing splitting of the nucleation mode and the soot mode for data analysis. This was done by taking the logarithm of the mobility diameter x-axis and fitting the data to a two-term gaussian model using Matlab Curve Fitting Toolbox. The fit parameters to the equation

$$y = a_1 \cdot \exp(-((x - b_1)/c_1)^2) + a_2 \cdot \exp(-((x - b_2)/c_2)^2)) \quad (3.1)$$

were then provided, allowing for analysis of the two modes as well as providing the R^2 for the fit. The $dN/dlogD_p$ amplitudes are represented by a_1 and a_2, x is log(d) where d is the mobility diameter, b_1 and b_2 are the logarithm of the geometric mean diameter (GMD) of the respective mode, and c_1 and c_2 are the logarithm of the GSD. The fit was not done for the PSL reference aerosols.

3.1.3.2 Derivation of PSL SA from SMPS size distribution

The surface area concentrations ($\mu m^2/cm^3$) of the reference PSL aerosols were calculated from the SMPS data for comparison to the Partector 2 surface area measurement. Since both the nucleation mode and the PSL spheres are spherical, this was simply done by taking the area calculated for each size bin diameter multiplied by the number concentration in each size bin and summing over all the size bins. This can be written as

$$SA = \sum A(d_p) \cdot dN/dlogd_p(d_p) \cdot dlogd_p \quad (3.2)$$

where $A(d_p)$ is the area of a sphere with the mobility diameter d_p as diameter, $dN/dlogd_p(d_p)$ is the normalized concentration for a given mobility diameter size bin, and $dlogd_p$ is 1/64 since the SMPS uses 64 channels per decade. By multiplying with $dlogd_p$ the normalized concentration was converted into dN, the particle concentration for the size bin.

3.1.3.3 Derivation of PSL LDSA from SMPS size distribution

The LDSA concentrations ($\mu m^2/cm^3$) of the reference PSL aerosols were also calculated from the SMPS data for comparison to the Partector 2 LDSA measurement. This was done precisely as for the surface area only now the surface area has to be multiplied by the alveolar deposition probability. Equation 2.1 was used where the deposition probability is provided by the ICRP deposition fraction for the alveolar region described in Equation 2.2. The exact calculation is then

$$LDSA = \sum A(d_p) \cdot dN/dlogd_p(d_p) \cdot dlogd_p \cdot DF_{AL}(d_p) \quad (3.3)$$

where all the parameters are the same as in the surface area calculation except that it is weighted with the deposition fraction $DF_{AL}(d_p)$ for every mobility diameter.

3.1.4 **Naneos Partector 2**

The Partector 2 is the main measurement tool that the research questions revolve around. The Partector 2 provides information on particle number concentration, GMD, surface area concentration ($\mu m^2/cm^3$), and LDSA ($\mu m^2/cm^3$). The instrument provides a value every second of operation. To acquire a singular value for the use in further calculations, the average of the entire 12-minute measurement for every material and treatment was calculated.

3.1.5 **Naneos Partector TEM**

This older version of the Partector has a TEM grid that collects the particles after measuring them, for potential use in TEM analysis. Unlike the Partector 2, the Partector TEM only measures LDSA ($\mu m^2/cm^3$). Precisely like the Partector 2, instrument provides a value each second. To acquire a singular value for the use in further calculations, the average of the entire 12-minute measurement for every material and treatment was calculated.

3.1.6 **Aethalometer**

The microAeth MA300 from Aethlabs was used to determine the eBC mass concentration. The infrared light (880 nm) was used with DualSpot loading compensation that corrects for optical loading effects. The microAeth

MA300 provides an average over every 30 seconds of operation. To acquire a singular value for the use in further calculations, the average of the entire 12-minute measurement for the soot and carbon black aerosols for both treatments were calculated.

3.1.7 **Measuring time and flow**

All the aerosols were measured for 12 minutes, to allow for 5 whole scans from the SMPS.

The flow to the different instruments were measured by a TSI Mass Flow Meter 41401 (0.01-20 L/min). The total flow of the set-up was 1.465 L/min. The flow to the Partector 2 was 0.535 L/min, 0.458 L/min to the Partector TEM, 0.157 L/min to the Aethalometer, and 0.275 L/min to the SMPS.

3.2 Partector 2 specific surface area (SSA)

The specific surface area (m^2/g) of the aerosols were calculated by dividing the Partector 2 average surface area concentration by the microAeth average eBC mass concentration. It should be noted that the surface area used in this case include both nucleation mode (NM) and soot mode (SM) of the aerosol since this is what the Partector 2 measures.

3.2.1 **Nucleation mode correction of Partector 2 surface area**

In this section the method of estimating a Partector 2 surface area that only includes the soot mode of the aerosol is described.

The surface area (SA) concentration measured by the Partector 2, as previously mentioned, contain both the nucleation mode (NM) and the soot mode (SM). One way of acquiring a value for only the soot mode could be simply removing the value measured during the deionized water measurement. However, the SMPS size distributions clearly show that the nucleation mode during the soot aerosol measurements were significantly different than during the deionized water measurement. This suggested that a better way of correction for the nucleation mode might be applied that takes into account both the size of the nucleation mode measured by the

SMPS and the surface area of the deionized water measurement from the Partector 2. The method chosen was to utilize the SMPS nucleation mode for every aerosol by calculating the surface area from the SMPS nucleation mode, which can be done since the particles in the nucleation mode are assumed to be spherical. However, the surface area calculated from the SMPS for deionized water are not the same as those measured by the Partector 2. Therefore, a correction constant was determined by plotting the surface area from the two methods against each other using both the untreated and the thermodenuded deionized water aerosols, see Figure 3.4.

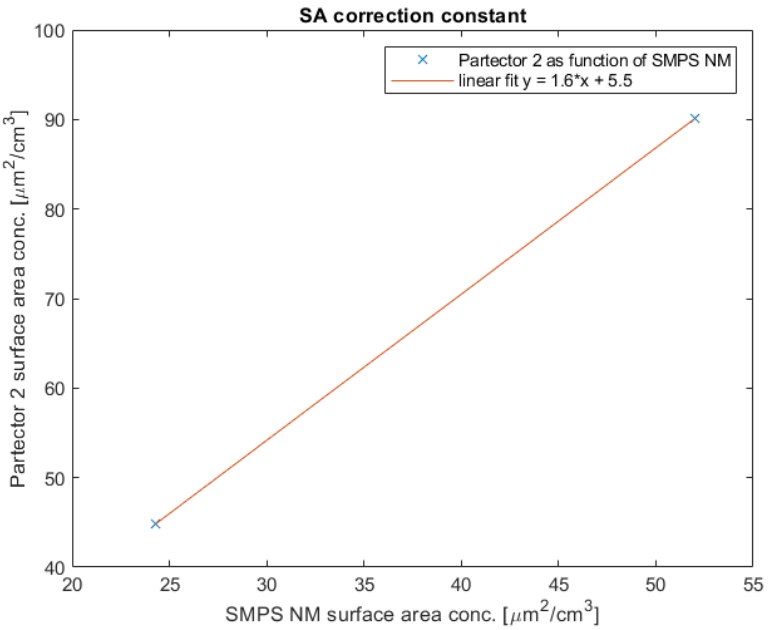

Figure 3.4 The nucleation mode correction factor, extracted from the slope of the Partector 2 vs SMPS nucleation mode for deionized water.

This means that the corrected Partector 2 surface area (SA^c) with the nucleation mode subtracted is given by

$$SA^c = SA_{Partector} - k_{SA} \cdot SA_{NM} \tag{3.4}$$

where $SA_{Partector}$ is the Partector 2 surface area concentration, $k_{SA} = 1.6$ is the correction factor extracted from Figure 3.4, and SA_{NM} is the calculated surface area concentration of the nucleation mode from the SMPS for a given aerosol.

3.2.2 **Derivation of mass concentration from effective density**

In this section the derivation of an alternative way of determining the soot mass to the Aethalometer is described using the effective density described in section 2.6. The calculation of the aerosol SSA using the Partector 2 surface area, and the soot mass acquired by the effective densities is also described.

The soot mass concentration was also calculated from the SMPS soot mode fit by using the effective density determined by Gysel et al. (2011) for Fullerene soot and Aquadag. The effective densities of Fullerene soot and Aquadag were found in literature, and for the rest of the materials an approximation was used instead which is the average of the affective density for Fullerene soot and Aquadag, see Figure 2.2. The soot mass concentration was then calculated from the SMPS soot mode as follows

$$BC_{eff} = \sum V(d_p) \cdot dN/dlogd_p(d_p) \cdot dlogd_p \cdot \rho_{eff}(d_p) \quad (3.5)$$

where $V(d_p)$ is the sphere volume from the mobility diameter, and $\rho_{eff}(d_p)$ is the effective density for each mobility diameter.

The SSA was then calculated from the Partector 2 surface area concentration divided by the soot mass concentration based off the effective density and SMPS soot mode for all the aerosols, as well as when using the corrected Partector 2 surface area concentration with the subtracted nucleation mode.

3.3 BET surface area analysis

BET analysis of the carbon blacks and soot were performed as reference for SSA. Since the amount needed for BET analysis (around 100 m^2) is rather large, the carbon black and soot were used directly from the powder instead of dispersing, nebulizing and collecting the aerosol.

The BET reference measurements were performed using a Micromeritics 3Flef surface characterization analyser, shown in Figure 3.5. The carbon black and soot powders were weighed on weighing papers and placed in a vial. To deal with the nuisance of electrostatic charge, the weighing paper, the scooping tool, and the vial were pre-treated with an ion fan. The samples were then pre-treated in a Micromeritics Smart VacPrep machine (shown in Figure 3.5) by applying vacuum and heating to 60 °C (300 °C for

the Aquadag to be able to remove the liquid it is in) to remove any adsorbed contaminants from the atmosphere such as water, after which the vial was filled with nitrogen gas. After the pre-treatment the samples were weighed again and attached to the 3Flex surface characterization analyser. There the sample was cooled in liquid nitrogen to roughly -196 °C. The adsorbent (i.e., nitrogen gas) was then introduced in well-defined doses, and by continually measuring the pressure the surface area of the sample can be calculated as previously described in the theory (section 2.7).

Figure 3.5 On the left: Micromeritics 3Flex surface characterization analyser used for BET reference measurement. On the right: Micromeritics Smart VacPrep used to pretreat samples for the 3Flex.

4 Results and discussion

4.1 BET SSA

In this section the reference BET SSA measurement results are presented, as well as a test that was performed to acquire how little soot was required for accurate BET surface area analysis.

The surface area of all four carbon blacks and one combustion soot mentioned in this thesis, were characterized using a micromeritics 3Flex surface area analyzer. The ethylene soot was not characterized due to an accident during the BET analysis and insufficient material to do another analysis. Due to problems with the weighing of the sample, the weight difference of the sample before and after the pre-treatment of the samples could not be used (unrealistic changes, such as negative values). Therefore, the weight of the sample before the pre-treatment was used for all but one of the samples in the BET surface area calculation. In an ideal case, the weight after the pre-treatment of the sample would be used as contaminants such as water are removed, and the removed weight should not be included in the BET surface area calculation. In the case of Aquadag the weight after pre-treatment was used, since the large amount of water removed cannot be allowed to contribute to the weight.

4.1.1 **BET sensitivity**

To determine how much material was needed to perform an accurate BET surface area measurement, the Fullerene soot was measured in different quantities and compared. The result of the different quantities of the Fullerene soot can be seen in Figure 4.1.

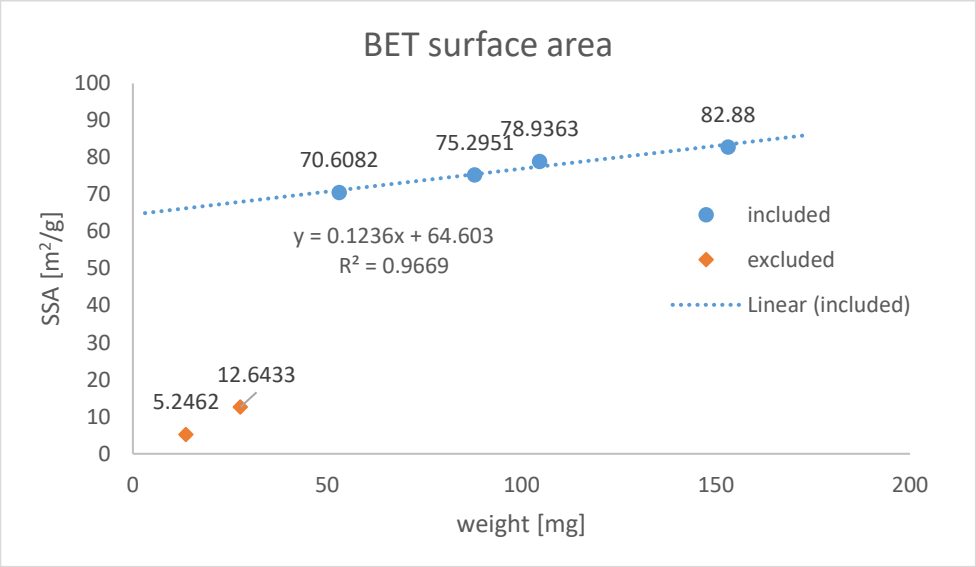

Figure 4.1 BET specific surface area measurement of different quantities of Fullerene soot. On the Y axis specific surface area is presented and on the X axis weight of the sample.

The measurements performed with less than 50 mg of Fullerene soot clearly did not have enough material to give an accurate measurement, evident by the much lower measured surface area. However, just above 50 mg the measurements seem to be in a similar size range, with an error estimate ±6.6 % with a 95 % confidence interval. It was also noticeable that there seems to be an almost linear dependence on sample mass for the measured surface area for the remaining measurements. Since one would expect a flat line when measuring the same material and not an increasing linear dependency with the amount of material used when measuring SSA (m^2/g), this could indicate either that too little material was used in all the measurements or that there is a systematic error in the measurement technique. However, in this thesis, it was concluded that quantities more than 50 mg appear to be sufficient to measure SSA of the soot powders within a reasonable error (~±6.6 %).

4.1.2 **BET SSA**

After establishing the quantity needed for accurate BET surface area analysis, the rest of the carbon blacks and soot were also measured with BET surface area analysis, see Figure 4.2. Regal carbon black R400 was measured with 953.8 mg, Printex 90 with 92.5 mg, miniCAST with 16.6

mg, and Aquadag with 75.3 mg after the liquid was removed. For the Fullerene soot the average of measurements with sufficient quantity from section 4.1.1 was used. Note that the ethylene soot was not able to be measured and that the miniCAST soot mass was insufficient for a reliable measurement according to the finding in the previous section.

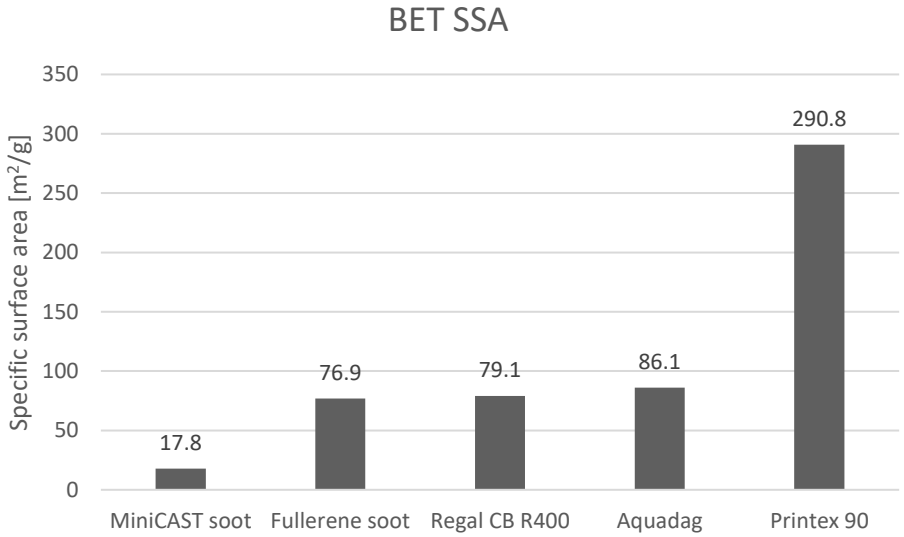

Figure 4.2 BET specific surface area of the different materials. Ethylene soot is not included due to insufficient material**.**

According to the manufacturer, Printex 90 has a BET surface area of 350 m^2/g (Specialty Carbon Blacks, 2019). The measured value of 290.8 m^2/g in Figure 4.2 is lower. This could be due to a different batch or the age of the sample (2018). There is also an uncertainty in the SSA of the Fullerene soot ±6.6 % with a 95 % confidence interval, found in the previous section.

4.2 Partector SSA and LDSA

In this section the results of the aerosols measurements are presented as well as the SSA and LDSA calculations.

All the aerosols measured in the aerosol lab were measured both untreated (UT) by bypassing the thermodenuder, and thermodenuded at 300 °C (TD). Each aerosol was measured for approximately 12 minutes. This allowed

good data statistics with the Partector 2, Partector TEM, Aethalometer, and five SMPS scans for each measurement set-point.

4.2.1 **Partector and Aethalometer measurement**

The average surface area concentration and average LDSA concentration measured by the Naneos Partector 2, as well as the average LDSA concentration measured by the Naneos Partector TEM, are presented in Table 4-1. The average eBC mass concentrations of the aerosols were measured by the Aethlabs microAeth MA300 are presented in Table 4-1.

Table 4-1 Measured data of all the aerosols from Partector 2, Partector TEM, and microAeth MA300. The values are an average of the 12-minute measurement. The values in the brackets are the standard deviations.

Material and treatment	**Partector 2 SA conc. ($\mu m^2/cm^3$)**	**microAeth eBC mass conc. (ng/m^3)**	**Partector 2 LDSA conc. ($\mu m^2/cm^3$)**	**Partector TEM LDSA conc. ($\mu m^2/cm^3$)**
Deionized water UT	90.1 (±1.9)	N/A	63.4 (±1.3)	77.2 (±2.2)
Deionized water TD	44.8 (±2.5)	N/A	31.5 (±1.8)	38.8 (±2.7)
Printex 90 UT	570.5 (±5.5)	6.6e4 (±2.3e3)	288.1 (±2.4)	345.2 (±8.2)
Printex 90 TD	435.3 (±10.5)	5.3e4 (±1.5e3)	213.8 (±3.9)	256.1 (±7.8)
Fullerene soot UT	1664.5 (±9.5)	9.0e4 (±2.8e3)	741.3 (±2.8)	852.2 (±10.8)
Fullerene soot TD	1292.7 (±11.3)	7.8e4 (±2.6e3)	541.2 (±4.9)	615.7 (±10.8)
Aquadag UT	1200.1 (±9.2)	18.7e4 (±4.7e3)	533.4 (±3.6)	612.5 (±6.3)
Aquadag TD	895.7 (±5.5)	14.3e4 (±4.3e3)	375.1 (±2.4)	420.4 (±5.5)
Regal CB R400 UT	704.1 (±14.2)	6.0e4 (±4.5e3)	340.6 (±5.0)	382.1 (±5.0)
Regal CB R400 TD	524.0 (±9.4)	4.3e4 (±1.9e3)	230.1 (±4.4)	258.5 (±6.2)
Ethylene soot UT	541.8 (±4.5)	6.8e4 (±1.4e3)	226.8 (±0.8)	257.4 (±4.6)
Ethylene soot TD	428.3 (±4.4)	6.0e4 (±2.6e3)	156.1 (±2.0)	174.4 (±4.1)
MiniCAST soot UT	1213.1 (±7.4)	7.5e4 (±2.1e3)	622.1 (±3.1)	726.3 (±8.0)
MiniCAST soot TD	964.8 (±4.7)	6.1e4 (±2.0e3)	467.5 (±3.1)	543.2 (±7.1)

When comparing the LDSA measured by the Partector 2 and the Partector TEM in Table 4-1, it became apparent that the Partector 2 consistently measures a slightly lower value for the same aerosol than the Partector

TEM. It was also clearly be seen that all measured data from the Partector 2, Partector TEM, and microAeth were lower after an aerosol passes through the thermodenuder. This is mainly because of thermophoresis and diffusion losses. Thermophoresis is a force exerted on the particles due to the temperature gradient present in the thermodenuder, causing a loss in particles.

4.2.2 **SMPS size distribution and fit**

The size distributions measured by the SMPS for the deionized water aerosols as well as the log normal fits are shown in Figure 4.3 and the fit parameters are presented in Table 4-2. The size distributions measured by the SMPS for the soot and black carbon aerosols as well as the log normal fits are shown in Figure 4.4, the fit parameters are presented in Table 4-2.

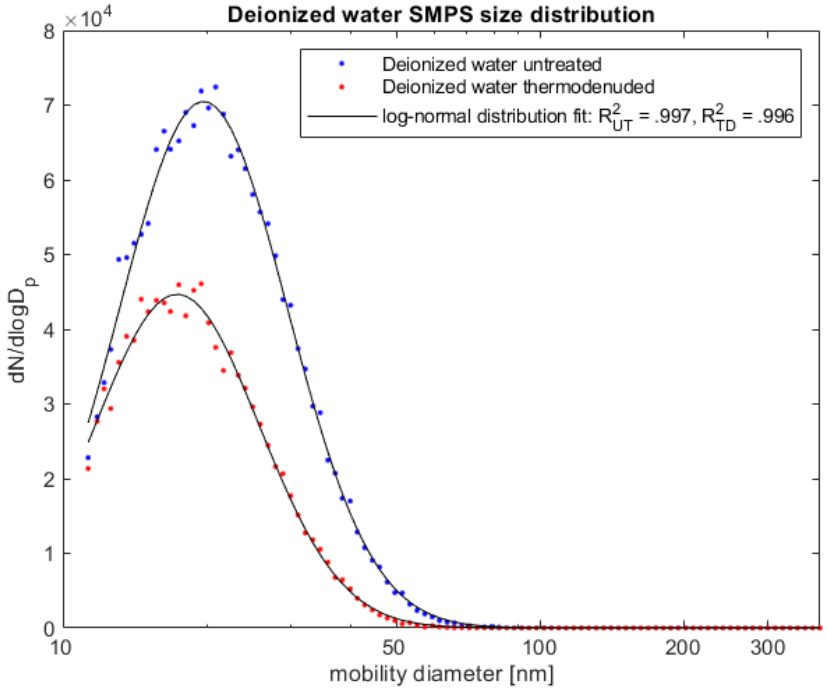

Figure 4.3 SMPS size distribution and log-normal fit for the untreated and thermodenuded deionized water aerosol.

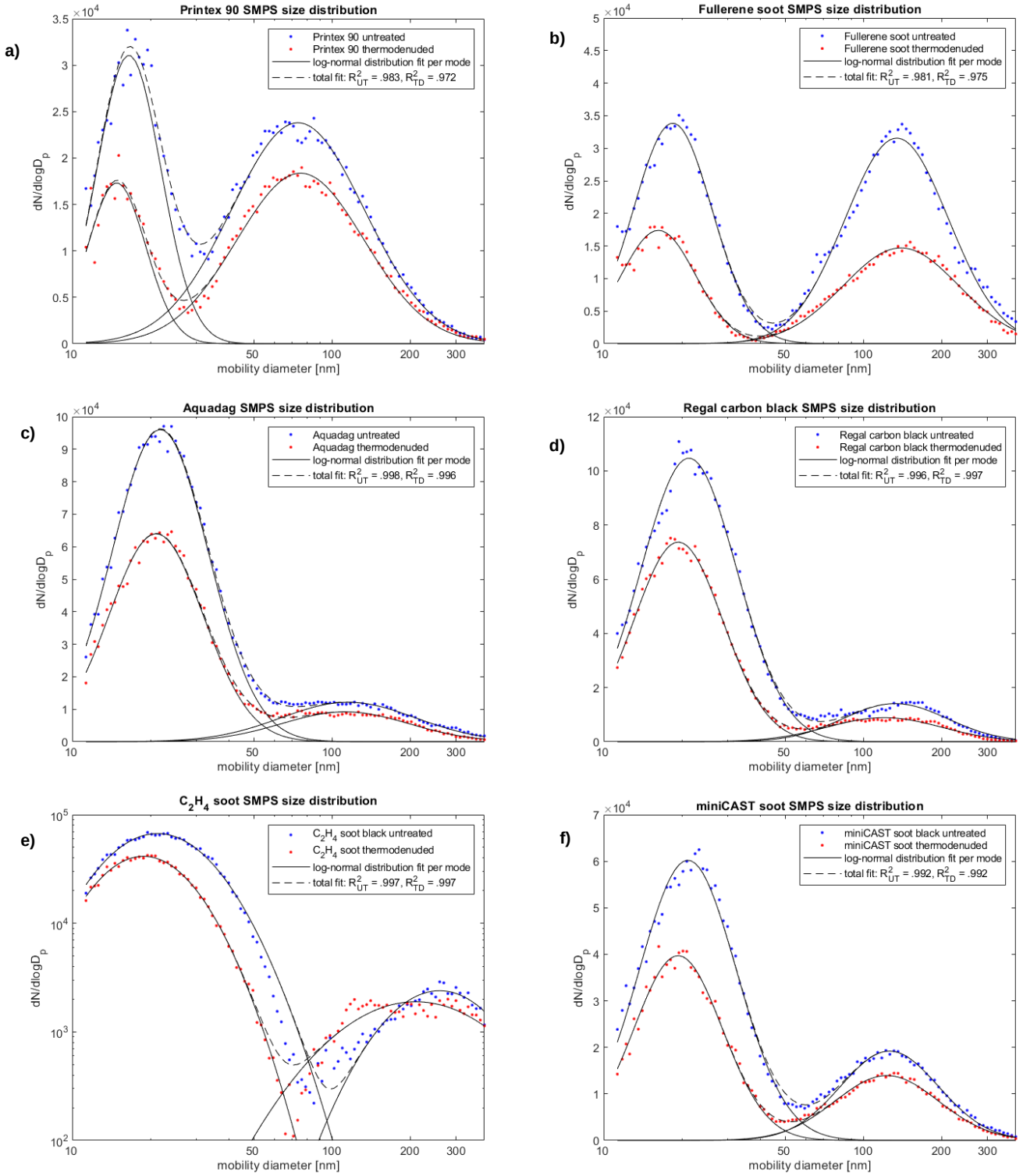

Figure 4.4 SMPS size distributions and log-normal fit for the untreated and themodenuded soot aerosols: a) Printex 90 b) Fullerene soot c) Aquadag d) Regal carbon black R400 e) Ethylene (C_2H_4) soot f) miniCAST mixed soot.

Table 4-2 Log-normal fit parameters of number (dN), geometric mean diameter (GMD), and geometric standard deviation (GSD) for the nucleation mode (NM) and soot mode (SM) of the SMPS data of all the aerosols.

Material and treatment	NM dN	NM GMD (nm)	NM GSD	SM dN	SM GMD (nm)	SM GSD	R^2
Deionized water UT	1100	19.7	1.8	NA	NA	NA	.997
Deionized water TD	700	17.4	1.8	NA	NA	NA	.996
Printex 90 UT	480	16.5	1.5	370	73.9	2.3	.983
Printex 90 TD	270	14.8	1.4	290	75.6	2.2	.972
Fullerene UT	530	18.5	1.6	490	134.3	1.9	.981
Fullerene TD	270	16.3	1.6	230	139.4	2.1	.975
Aquadag UT	1500	21.8	1.8	190	115.4	2.3	.998
Aquadag TD	1000	21.0	1.8	140	112.3	2.2	.996
Regal CB R400 UT	1640	21.3	1.8	220	132.4	1.9	.996
Regal CB R400 TD	1150	19.4	1.8	140	120.1	2.0	.997
Ethylene soot UT	1050	21.3	1.8	40	259.0	1.8	.997
Ethylene soot TD	650	18.8	1.7	30	209.8	2.3	.997
MiniCAST soot UT	940	21.1	1.8	300	125.8	1.9	.992
MiniCAST soot TD	620	19.4	1.7	220	123.0	1.9	.992

When looking at the SMPS size distributions for the soot aerosols, the most obvious thing seen was that there are two modes present. The mode around 20 nm was in the same place as for the size distribution for deionized water and is known to be the nucleation mode (NM). Interestingly, the nucleation mode was not identical for every aerosol, although similar enough to be clearly distinguishable.

The soot mode is the mode at larger size that was only present for the soot aerosols and completely absent for the deionized water mode.
The number concentration of the aerosols was significant lower when the aerosol passes through the thermodenuder compared to when untreated going through the bypass tube, mainly as a result of thermophoresis and diffusion losses. After passing through the thermodenuder the shape of the size distribution looks to be relatively unchanged, except for the mentioned loss in number concentration, and a slight variation in average particle diameter, see Table 4-2. In this Table, the values given are those of the log-

normal fit for the nucleation mode and soot mode of the SMPS size distributions. The high R^2 gives good confidence in the fitted log-normal distributions and is visually clear in Figure 4.4.

It is noticeable that the magnitude of the nucleation mode number concentration was the same as the magnitude of the soot mode for most of the aerosols. This is not ideal because it provides unwanted "noise" for the soot measurements, however, since the particles are so small in the nucleation mode, the impact on surface area and LDSA will be relatively much lower. The reason for the high number concentration of the nucleation mode was most likely due to the deionized water not being clean enough. Another reason could be that the lab equipment, such as the tubing and instruments, not being clean enough. The latter was rejected because the equipment gave near zero reading when testing the set-up with a clean air flow when not nebulizing an aerosol.

4.2.3 **PSL sphere SA and LDSA validation**

In this section the SA concentration and LDSA concentration of the reference PSL spheres from the Partector 2/TEM are presented alongside the calculated values from the SMPS data as described in section 3.1.3.2-3. The values are then compared and discussed.

The SA and LDSA can be calculated from the PSL sphere aerosol SMPS data because all particles can be assumed to be spherical. The resulting SA and LDSA concentrations are presented in Table 4.3 and shown in Figure 4.5-7.

Table 4-3 Surface area (SA) and LDSA from Partector 2 measurement of the PSL spheres as well as LDSA from the Partector TEM, in addition to calculated SA concentration and LDSA concentration of the PSL sphere aerosols from the SMPS size distributions. The values in the brackets are the standard deviations.

Material and treatment	Partector 2 SA conc. ($\mu m^2/cm^3$)	SMPS SA conc. ($\mu m^2/cm^3$)	Partector 2 LDSA conc. ($\mu m^2/cm^3$)	Partector TEM LDSA conc. ($\mu m^2/cm^3$)	SMPSxICRP LDSA conc. ($\mu m^2/cm^3$)
PSL 220 nm UT	235.7 (±4.1)	166.4	156.6 (±2.5)	187.4 (±4.0)	35.4
PSL 220 nm TD	154 (±1.4)	110.9	102.3 (±0.5)	122.9 (±2.7)	23.1
PSL 269 nm UT	751.5 (±2.8)	491.0	496.8 (±1.7)	582.8 (±5.2)	144.4
PSL 269 nm TD	273.8 (±3.0)	194.2	192.7 (±2.1)	233.4 (±2.1)	57.6

PSL 350 nm UT	170.6 (±1.1)	117.0	120.1 (±0.7)	150.8 (±3.3)	29.9
PSL 350 nm TD	130.2 (±0.5)	116.8	91.6 (±0.3)	114.7 (±2.6)	25.0

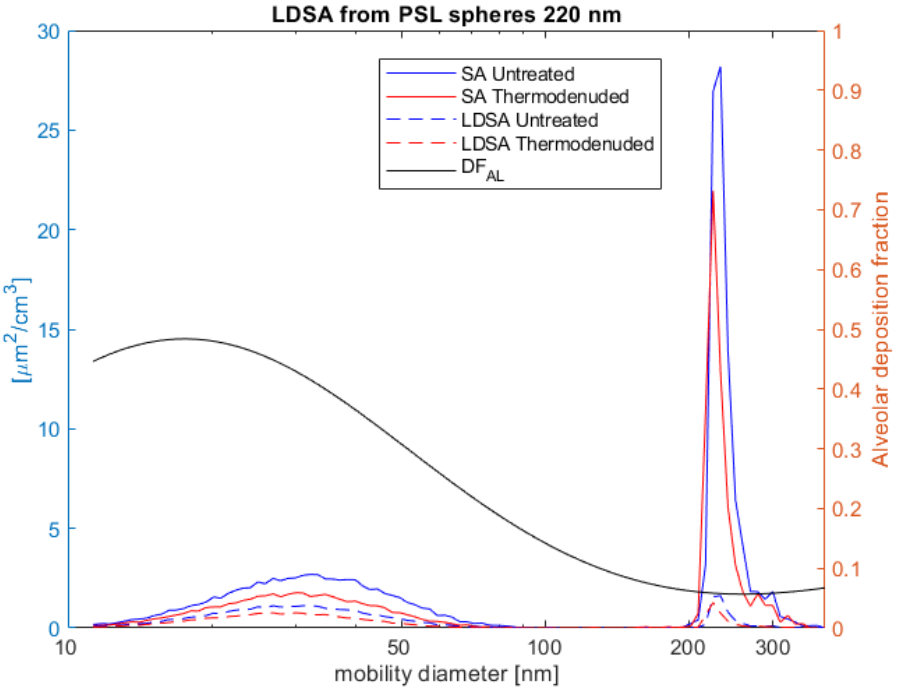

Figure 4.5 220 nm PSL sphere aerosol surface area concentration and LDSA concentration obtained from the ICRP alveolar deposition fraction.

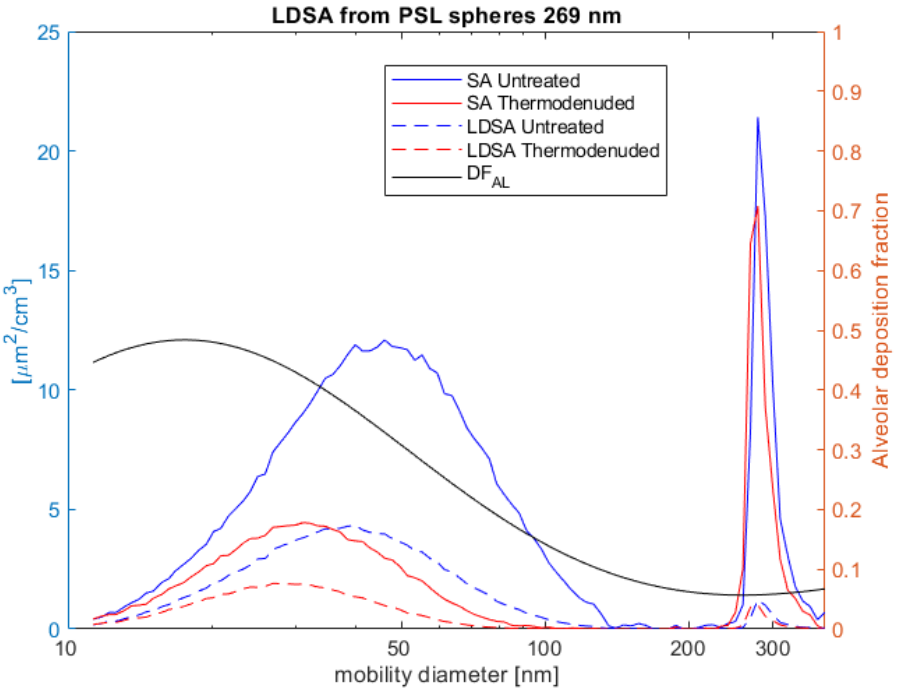

Figure 4.6 269 nm PSL sphere aerosol surface area concentration and LDSA concentration obtained from the ICRP alveolar deposition fraction.

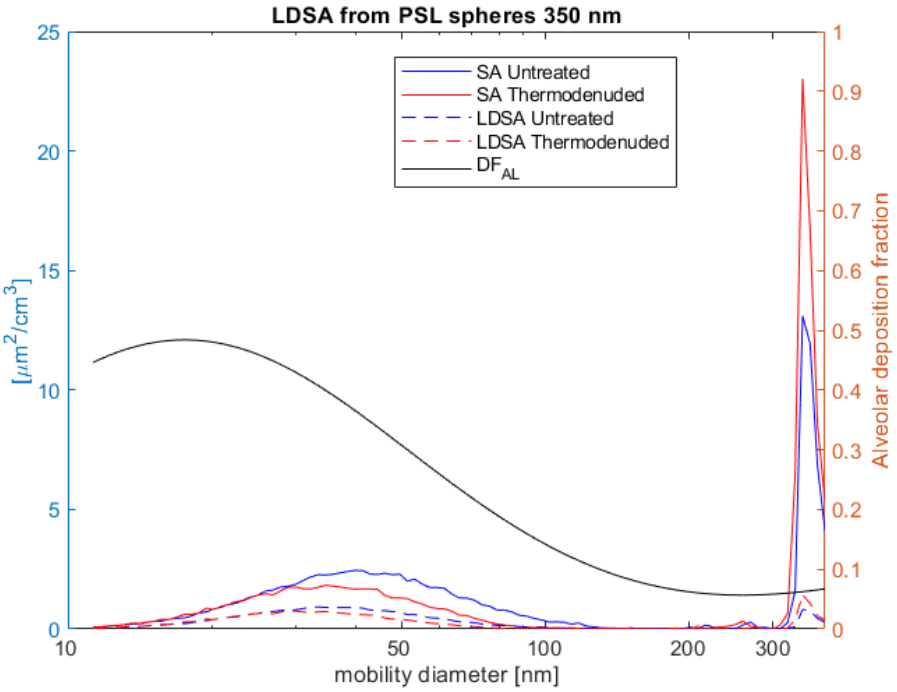

Figure 4.7 350 nm PSL sphere aerosol surface area concentration and LDSA concentration obtained from the ICRP alveolar deposition fraction.

In Figures 4.5-7 it was observed that the LDSA measured from the nucleation mode was larger than the LDSA from the PSL sphere peak. This is unfortunate and origin from the large nucleation mode compared to small number of PSL spheres measured. This will be a limitation for the conclusions drawn by these measurements.

When looking at the surface area concentration of the PSL spheres measured by the Partector 2 it was observed that on average it was 38.7 % (± 11.9 % with 95 % confidence interval) higher than the surface area concentrations determined from the SMPS size distributions in Table 4-1. When plotted against each other, see Figure 4.8, a good linear fit (R^2 = .997) was found. This shows that the Partector 2 and the SMPS measurements are well correlated and that the value increases linearly with increased surface area measured. However, the Partector 2 data must be corrected with the scaling factor (i.e., 1.59, see Figure 4.8).

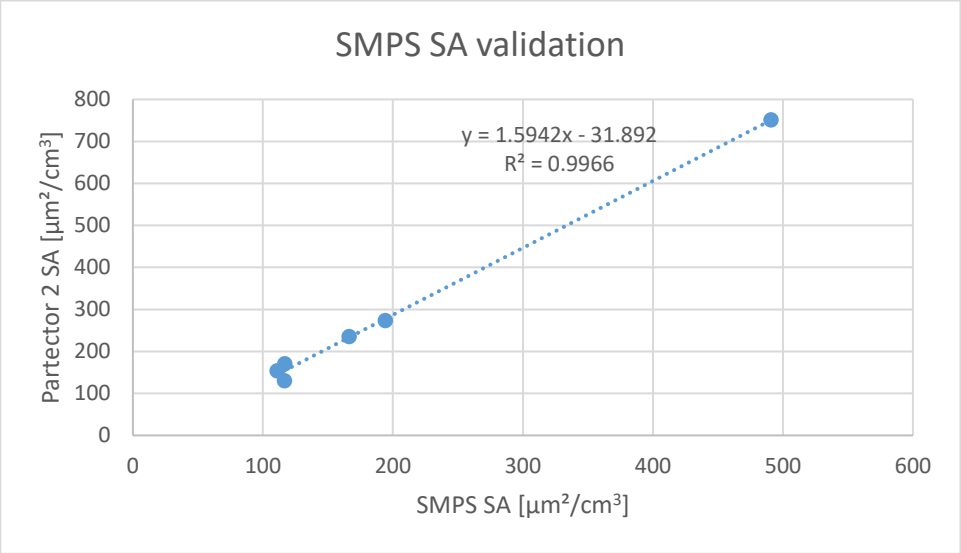

Figure 4.8 Validation of the Partector 2 surface area (SA) concentration against the SMPS surface area (SA) concentration.

When instead looking at the LDSA concentrations of the PSL spheres, it was seen that the Partector 2 measures a 288.6 % (± 40.0 % with 95 % confidence interval) higher value on average than that determined by the SMPS size distributions and the ICRP alveolar deposition fraction. This is very interesting as one would expect that the surface area and LDSA values from the two methods would differ by around the same percentage. The manufacturer of the Partector 2 state that the LDSA measured by the instrument is overstated for small particles, especially below 20 nm, and understated for larger particles, especially above 350 nm (Lung-deposited surface area, 2021). This could be one of the reasons behind the larger LDSA measurement from the Partector 2 since most of the surface area calculated by the SMPS size distribution for the PSL aerosols is from the PSL peaks at 220 nm, 269 nm, and 350 nm, and a lesser portion from the nucleation mode peak with a mean of approximately 20 nm. Another reason for the discrepancy could arise from the assumption made that the nucleation mode particles are spherical. This assumption may not be entirely true, however this would affect both the surface area and LDSA values. When plotted against each other, see Figure 4.9, a good linear fit (R^2 = .993) was found as well that indicates that the Partector 2 and the SMPS measurements, just like for the surface area, were well correlated but with a linear dependence set apart from the expected 1:1.

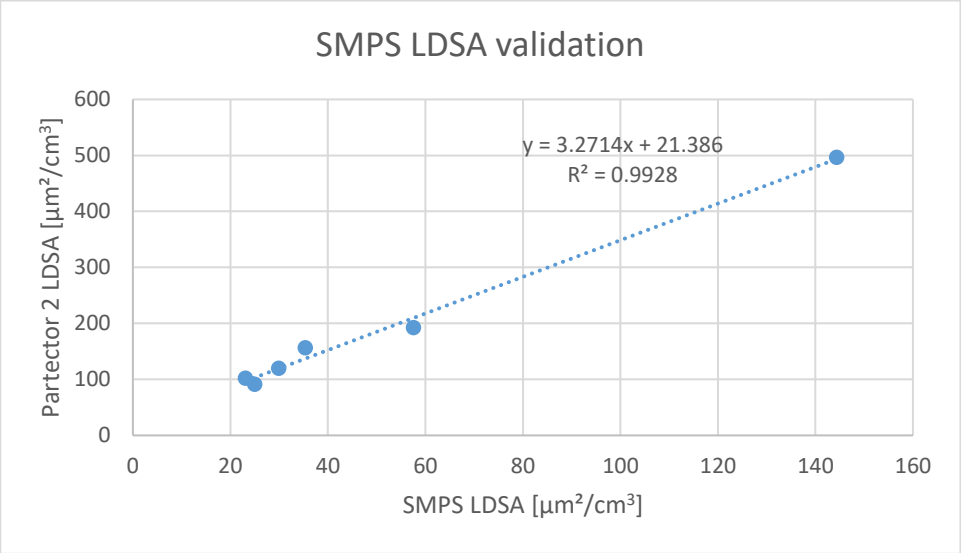

Figure 4.9 Validation of the Partector 2 LDSA concentration against the SMPS LDSA concentration.

From Figure 4.8 and Figure 4.9, it was concluded that the Partector 2 measures surface area and LDSA that is proportional to the surface area measured by SMPS for spherical particles but with a scaling factor.

Another interesting thing to mention is that since the PSL sphere peaks in the SMPS size distributions are mostly unaffected by the thermodenuder, the discrepancy between the untreated and thermodenuded PSL aerosol measurements are almost entirely due to the reduced nucleation mode after passing through the thermodenuder.

An outlier in the PSL sphere aerosols was the untreated 269 nm that shows considerably higher Partector 2 SA concentration (751.5 $\mu m^2/cm^3$), Partector 2 LDSA concentration (496.8 $\mu m^2/cm^3$), and Partector TEM LDSA concentration (582.8 $\mu m^2/cm^3$) than the other PSL sphere measurements. This was caused by the nucleation mode for this aerosol being a lot bigger than for the other PSL sphere aerosols, seen in the SMPS size distributions for the PSL sphere aerosols, see Appendix A.

4.2.4 **Nucleation mode correction and effective density calculation**

Using the SMPS log-normal fit for the nucleation mode of the size distribution and assuming that the particles in the nucleation mode are spherical as described in section 3.2, the SA concentration of the SMPS (SA_{NM}) was calculated for the soot aerosols, see Table 4-4. Using the SA_{NM} and the correction factor k_{SA} described and calculated in section 3.2, a corrected value of the Partector 2 surface area concentration was determined that subtracts the nucleation mode surface area, see the result in Table 4-4. The mass concentration of the soot aerosols that were calculated by using the SMPS soot mode fit, and the effective density as described in section 3.2 are presented in Table 4-4. Note that the effective density for Aquadag and Fullerene soot was found in literature whilst the effective density of the rest of the soot's were approximated by taking an average value of the Aquadag and Fullerene soot effective densities.

Table 4-4 Calculated values used in further calculations. The SA concentration calculated from the SMPS NM fit SA_{NM}, the corrected SA concentration from the Partecor 2 SA^c, and the mass concentration obtained by the SMPS SM and the effective density.

Material and treatment	**SA_{NM} conc. ($\mu m^2/cm^3$)**	**SA^c conc. ($\mu m^2/cm^3$)**	**mass conc. from SMPS SM and ρ_{eff} (ng/m^3)**
Deionized water UT	52.0	N/A	N/A
Deionized water TD	24.3	N/A	N/A
Printex 90 UT	9.4	555.4	9383.2
Printex 90 TD	3.6	429.5	6864.3
Fullerene soot UT	17.3	1636.8	28431.5
Fullerene soot TD	6.2	1282.8	16878.5
Aquadag UT	95.4	1047.5	12625.2
Aquadag TD	57.0	804.4	8231.9
Regal carbon black UT	98.1	547.1	12530.7
Regal carbon black TD	50.3	443.5	7507.6
C2H4 soot UT	64.1	439.2	5411.6
C2H4 soot TD	26.1	386.6	4274.1
MiniCAST soot UT	56.8	1122.2	13577.2
MiniCAST soot TD	26.6	922.3	10361.0

4.2.5 **Specific surface area calculations and validation**

The specific surface area of the aerosols was calculated using the Partector 2 surface area concentration and the equivalent black carbon mass concentration (SSA_{eBC}) as described in section 3.2, see Table 4-5. The specific surface area of the aerosols was also calculated using the corrected Partector 2 surface area concentration and the equivalent black carbon mass concentration (SSA^{c}_{eBC}) as described in section 3.2, see Table 4-5. The specific surface area of the aerosols was also calculated using the Partector 2 surface area concentration but with a different mass concentration acquired from the SMPS soot mode fits and the effective density (SSA_{eff}), as well as when using the corrected Partector 2 surface area concentration (SSA^{c}_{eff}), see Table 4-5.

Table 4-5 Specific surface area calculated from the Partector 2 surface area concentration and two methods of acquiring the soot mass concentration. eBC denotes the mass acquired from the aethalometer and eff the mass acquired from the SMPS soot mode fit and effective denity. The c denotes that the Partector 2 surface area was corrected for without the nucleation mode. For ease of comparison the BET specific surface area was also included, SSA_{BET}.

Material and treatment	**SSA_{eBC} (m^2/g)**	**SSA^{c}_{eBC} (m^2/g)**	**SSA_{eff} (m^2/g)**	**SSA^{c}_{eff} (m^2/g)**	**SSA_{BET} (m^2/g)**
Deionized water UT	N/A	N/A	N/A	N/A	N/A
Deionized water TD	N/A	N/A	N/A	N/A	N/A
Printex 90 UT	8.7	8.4	60.8	59.2	290.8
Printex 90 TD	8.3	8.2	63.4	62.6	N/A
Fullerene soot UT	18.6	18.3	58.5	57.6	76.9
Fullerene soot TD	16.6	16.5	76.6	76.0	N/A
Aquadag UT	6.4	5.6	95.1	83.0	86.1
Aquadag TD	6.3	5.6	108.8	97.7	N/A
Regal CB R400 UT	11.8	9.1	56.2	43.7	79.1
Regal CB R400 TD	12.1	10.3	69.8	59.1	N/A
Ethylene soot UT	8.0	6.5	100.1	81.2	N/A
Ethylene soot TD	7.1	6.4	100.2	90.5	N/A
MiniCAST soot UT	16.1	14.9	89.3	82.7	N/A
MiniCAST soot TD	15.9	15.2	93.1	89.0	N/A

When looking at the specific surface area calculated from the Partector 2 surface area concentration and the eBC mass concentration measured by the microAeth, see Table 4.5, the values were far lower than expected from the BET analysis. After removal of the nucleation mode contribution to the specific surface area (SSA^{c}_{eBC}) the values were slightly reduced, on average

to 90.9 % (± 4.5 % with 95 % confidence interval) of the uncorrected value (SSA_{eBC}).

When instead looking at the specific surface area calculated from the Partector 2 surface area concentration and the mass concentration calculated from the effective density and the soot mode fit from the SMPS size distribution the values were much more reasonable. When once again using the corrected Partector 2 surface area, the SSA was on average 91.1 % (± 4.5 % with 95 % confidence interval) of the non-corrected value.

To visualize the comparison between the specific surface area determined from the Partector 2 surface area concentration and the two methods of acquiring the mass concentration (untreated SSA^{c}_{eBC} and SSA^{c}_{eff}), to the reference specific surface area from BET analysis (SSA_{BET}), they were plotted against each other, see Figure 4.10. Note that the Ethylene and miniCAST soot were not included because it was not possible to perform BET analysis with sufficient mass for these samples. Only the values with corrected surface area were included as they are more relevant, and the discussion will hence forth be limited to these values. The dotted line in the figure shows the 1:1 line where the data points would be if the values were the same as the BET reference.

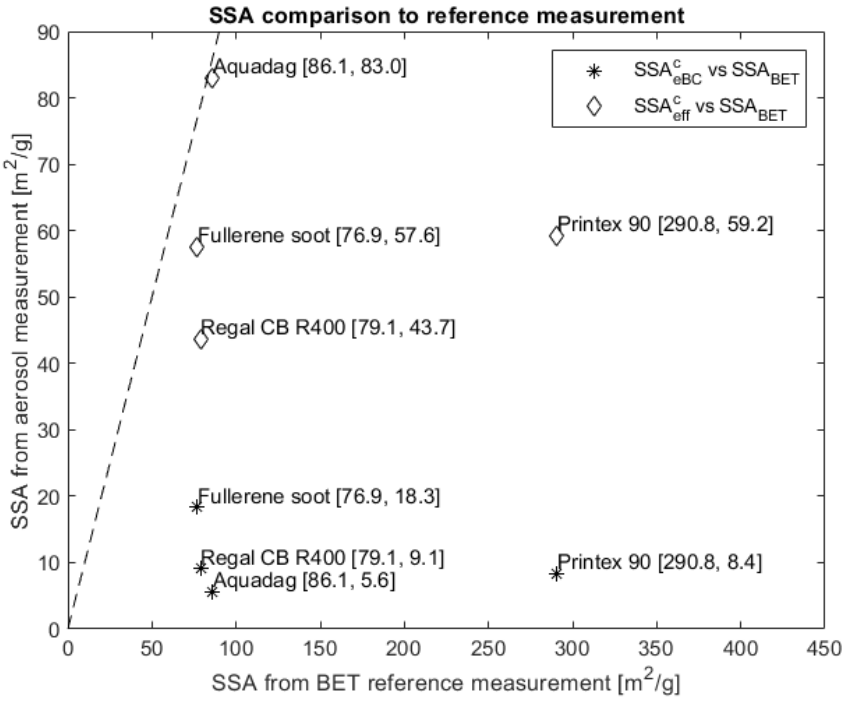

Figure 4.10 The two different calculated SSA from the aerosol measurement plotted against the reference SSA_{BET}. SSA^{c}_{eBC} is the SSA calculated from the corrected Partector 2 surface area concentration and the aethalometer eBC mass concentration. SSA^{c}_{eff} is the SSA calculated from the corrected Partector 2 surface area concentration and the mass concentration derived from the SMPS SM fit and the effective density. A dotted line represents a perfect 1 to 1 fit.

The untreated SSA^{c}_{eff} for Aquadag (83.0 m^2/g) and Fullerene soot (57.6 m^2/g) for which the effective densities were found in literature, were within ±30 % to that measured in the BET analysis (86.1 m^2/g and 76.9 m^2/g respectively). As seen in Figure 4.10 these two values were also the closest to the BET reference of all the measured soot. The third closest by a margin was the untreated SSA^{c}_{eff} for Regal carbon black R400 (43.7 m^2/g) which is almost half the specific surface area measured by BET (79.1 m^2/g). For Printex 90 the SSA^{c}_{eff} (69.2 m^2/g) was not a good measurement compared to the SSA_{BET} (290.8 m^2/g). The deviation could potentially be explained if the assumption that the effective density of Printex 90 was similar to Aquadag and Fullerene soot was wrong.

As previously mentioned, the untreated SSA^{c}_{eBC} values were all extremely low. Aquadag (5.6 m^2/g), Fullerene soot (18.3 m^2/g), Regal carbon black

R400 (9.1 m^2/g), and Printex 90 (8.4 m^2/g) were both much lower than the reference SSA_{BET} as well as considerably lower than SSA^c_{eff}. This is visually clear in Figure 4.10. Because the surface area measured by the Partector 2 were used for both SSA^c_{eBC} and SSA^c_{eff}, this indicates that the aethalometer eBC concentration was not a reliable soot particle mass estimate in the conducted experiment.

4.2.6 **Thermodenuder and organic carbon**

In this section a comparison between the soot aerosols passing though the thermodenuder to the untreated aerosols will be made.

It was difficult to see how the soot particles are affected by the thermodenuder. From the SMPS data it was clear that the number concentration of particles in both the nucleation mode and the soot mode decreased after passing through the thermodenuder. This was mainly because of thermophoresis and diffusion losses. A loss in particles should not affect the specific surface area of the soot particles, however, the removal of volatile compounds such as organic carbon might. The SSA^c_{eBC} after passing through the thermodenuder was on average 100.2 % (± 6.3 % with 95 % confidence interval) of the value for the untreated aerosols. When looking at the more reasonable SSA^c_{eff}, it was on average 118.3 % (± 10.5 % with 95 % confidence interval) of the value of the untreated aerosols after passing through the thermodenuder. If the discussion is kept to the latter, it could be concluded that the specific surface area of the soot particles increase after the volatile compounds on them were removed.

5 Conclusions and outlook

The specific surface area for four different carbon blacks (Aquadag, Fullerene soot, Printex 90, and Regal carbon black R400) were determined by calculation from the Partector 2 surface area concentration and the mass concentration acquired from two different methods, aethalometer eBC and SMPS size distribution together with the effective density. A reference SSA measurement was performed by BET analysis. It could be concluded that the aethalometer eBC concentration was not a reliable soot particle mass estimate for the measurements conducted in this thesis. With the soot mass concentration acquired from the effective density found in litterature, reasonable specific surface areas were acquired for Aquadag and Fullerene soot compared to that measured during BET surface area analysis (3.6 % and 25.1 % lower than BET respectively). For Regal carbon black R400 and Printex 90 where the effective densities were approximated, the specific surface areas acquired were far off the refence BET value (55.3 % and 79.6 % lower than BET), especially for the Printex 90.

The primary aim of this thesis was to validate the Partector 2 instrument and measurement of specific surface area on combustion related soot particles and engineered carbon black nanoparticles. The results in this thesis show that the Partector 2 surface area measurement for spherical particles was well correlated (R^2 = .997, n= 6), but with a scaling factor that potentially could be corrected for. The LDSA measured by the Partector 2 was also well correlated (R^2 = .993, n = 6) for spherical particles, but with an even bigger scaling factor. It was found that the specific surface area for engineered carbon blacks were in best agreement when measuring with the Partector 2 and using the sot mass found by the correct effective density and SMPS measurement (Fullerene soot and Aquadag). The two other carbon blacks investigated (Regal carbon black R400 and Printex 90) were very far off the BET reference value. Since only one of the four carbon black SSA was close to the BET reference (2.6 % off), the Partector 2 was not found to be accurate for engineered carbon black nanoparticles. It was

however indicated that there might be potential when the correct mass concentration is determined. If further calibration was made to the Partector 2 instrument, a more accurate surface area measurement could potentially be achieved, especially for spherical particles.

To further validate the Partector 2 instrument, TEM analysis could be performed on the collected particles from the Partector TEM. Determining SSA from TEM images of soot particles has been proven a reliable approach previously benchmarked towards BET analysis (Bourrous et al., 2018). A major advantage of this method was mentioned in the article to be when the amount of mass obtainable is too small for BET measurement.

An issue during all the aerosol measurements done in this thesis has been the high particle number in the nucleation mode from the deionized water. This could hopefully be largely improved with an even cleaner grade of deionized water. Another way to improve this could be to increase the length of the setup to cause more diffusion losses from the nucleation mode particles.

All the aerosols in this thesis were measured untreated (bypass) as well as passing through a thermodenuder. It could be concluded that the specific surface area of the soot particles increased after the volatile compounds on them were removed. To further improve this comparison, a measurement of the organic carbon present on the particles before and after the thermodenuder can be conducted.

The implication of this study is that the Partector 2 particle surface area measurement for spherical particles is linearly related to the reference surface area. The deviation from the true surface area can be adjusted for if the aerosol is pre-calibrated, and caution must therefore be taken when using the Partector 2 results in different environments. For non-spherical soot particles, the Partector 2 surface area measurement was less reliable when benchmarked towards BET analysis. However, the results in this thesis may be improved not only by improving the Partector 2 instrument, but also from more thorough soot mass measurements. Nonetheless, this study shows that for most of the particles analyzed by BET, SSAs derived from the combination of Partector 2, SMPS size distributions and assumptions of effective particle density were in reasonable agreement (±30%). The instrument could thus be a good tool for on-line measurements when the values reported are more used as an indication or relative

comparison, rather than an exact determination of surface area. Because of this and considering the excellent mobility of the device, it can very favorably be used for health-related measurements in for example workplace environments. Further testing and calibration of the Partector 2 instrument is however needed to reach its full potential.

References

Baron, P., Kulkarni, P., & Willeke, K. (2011). *Aerosol measurement: Principles, Techniques, and Applications* (3dr ed.). Hoboken, New Jersey: John Wiley & Sons, Inc..

Bourrous, S., Ribeyre, Q., Lintis, L., Yon, J., Bau, S., Thomas, D., Vallières, C., & Ouf, F. (2018). A semiautomatic analysis tool for the determination of primary particle size, overlap coefficient and specific surface area of nanoparticles aggregates. *Journal of Aerosol Science, 126*, 122-132. https://hal.archives-ouvertes.fr/hal-01877516

Ceresana. (2022). *Carbon Black Market Report*. Accessed May 23 2022. https://www.ceresana.com/en/market-studies/chemicals/carbon-black/

Dalirian, M., Ylisirniö, A., Buchholz, A., Schlesinger, D., Ström, J., Virtanen, A. & Riipinen, I. (2018). Cloud droplet activation of black carbon particles coated with organic compunds of varying solubility. *Atmospheric Chemistry and Physics 18*, 12477-12489. https://doi.org/10.5194/acp-18-12477-2018

DeCarlo, P., Slowik, J., Worsnop, D., Davidovits, P. & Jimenez, J. (2004).) Particle Morphology and Density Characterization by Combined Mobility and Aerodynamic Diameter Measurements. Part 1: Theory. *Aerosol Science and Technology, 38*(12), 1185-1205. https://doi.org/10.1080/027868290903907

Fierz, M., Meiner, D., Steigmeier, P., & Burtscher, H. (2014). Aerosol Measurement by Induced Currents. *Aerosol Science and Technology, 48*, 350-357. https://doi.org/10.1080/02786826.2013.875981

Guo, S., Hu, M., Peng, J., Wu, Z., Zamora, M., Shang, D., DU, Z., Zheng, J., Fang, X., Tang, R., Wu, Y., Zeng, L., Shuai, S., Zhang, W., Wang, Y., Ji, Y., Li, Y., Zhang, A., Wang, W., Zhang, F., Zhao, J., Gong, X., Wang, C., Molina, M. & Zhang, R. (2020). Remarkable nucleation and growth of ultrafine particles from vehicular exhaust. *Proceedings of the National Academy of Sciences, 117*(7), 3427-3432. https://doi.org/10.1073/pnas.1916366117

Gysel, M., Laborde, M., Olfert, J. S., Subramanian, R., & Gröhn, A. J. (2011). Effective density of Aquadag and fullerene soot black carbonreference materials used for SP2 calibration. *Atmospheric Measurement Techniques, 4*(12), 2851-2858. https://doi.org/10.5194/amt-4-2851-2011

Hinds, W. (1999). *Aerosol technology: properties, behaviour, and measurement of airborne particles* (2nd ed.). Los Angeles, California: John Wiley & Sons, Inc.

Kumfer, B. & Kennedy, I. (1991). The role of soot in health effects of inhaled airborne particles. Bockhorn, H., D'Anna, A., Sarofim, A. F. & Wang, H. *Combustion Generated Fine Carbonaceaous Particles*, (s. 1-15). Davis, CA. Univeristy of California.

Kuuluvainen, H., Rönkkö, T., Järvinen, A., Saari, S., Karjalainen, P., Lähde, T., Pirjola, L., Niemi, J., Hillamo, R., & Keskinen, J. (2016). Lung deposited surface area size distributions of particulate matter in different urban areas. *Atmospheric Environment, 136*, 105-113. https://doi.org/10.1016/j.atmosenv.2016.04.019

Lung-deposited surface area, naneos particle solutions gmbh, (2021). https://www.naneos.ch/pdf/LDSA.pdf

Maricq, M. (2007). Chemical characterization of particulate emissions from diesel engines: A review. *Journal of Aerosol Science 38*, 1079-1118. https://doi.org/10.1016/j.jaerosci.2007.08.001

microAeth MA series MA200, MA300, MA350 Operating Manual, AethLabs, (2018). https://aethlabs.com/sites/all/content/microaeth/maX/MA200%20MA300%20MA350%20Operating%20Manual%20Rev%2003%20Dec%202018.pdf

Micromeritics, Retrieved May 22, 2022. [figure] with permission. https://www.micromeritics.com/particle-testing/analytical-testing/surface-area/

Oberdörster, G., Oberdörster, E., & Oberdörster, J. (2005). Nanotoxicology: An Emerging Discipline Evolving from Studies of Ultrafine Particles. *Environmental Health Perspectives 113*(7), 823-839. https://doi.org/10.1289/ehp.7339

Partector 2 Operation Manual, Naneos, (2022). https://www.naneos.ch/pdf/naneos_partector2_operation_manual.pdf

Petzold, A., Ogren, J. A., Fiebig, M., Laj, P., Li, S.-M., Baltensperger, U., Holzer-Popp, T., Kinne, S., Pappalardo, G., Sugimoto, N., Wehrli, C., Wiedensholer, A. & Zhang, X.-Y. (2013). Recommendations for reporting "black carbon" measurements. *Atmospheric Chemistry and Physics, 13*, 8365-8379. https://doi.org/10.5194/acp-13-8365-2013

Speciality Carbon Blacks, Orion Engineered Carbons GmbH, Germany, (2019). https://www.orioncarbons.com/en/26_02_19_td_0112_farbrusstabelle_emea_web_1_1.pdf

Schmid, O., & Stoeger, T. (2016). Surface area is the biologically most efficient dose metric for accurate nanoparticle toxicity in the lung. *Journal of Aerosol Science*,

99, 133-143.
https://doi.org/10.1016/j.jaerosci.2015.12.006

Wilson, W., Stanek, J., Han, H., Johnson, T., Sakurai, H., Pui, D., Turner, J., Chen, D., & Duthie, S. (2007). Use of the Electrical Aerosol Detector as an Indicator of the Surface Area of Fine Particles Deposited in the Lung. *Journal of the Air & Waste Management Association*, *57*(2), 211-220
https://doi.org/10.1080/10473289.2007.10465321

World Health Organization (2021, September 22). *New WHO Global Air Quality Guidelines aim to save millions of lives from air pollution* [Press release]. Retrieved January 18, 2022, from https://www.who.int/news/item/22-09-2021-new-who-global-air-quality-guidelines-aim-to-save-millions-of-lives-from-air-pollution

World Health Organization (2021). *WHO global air quality guidelines.* https://apps.who.int/iris/bitstream/handle/10665/345329/9789240034228-eng.pdf?sequence=1&isAllowed=y

Appendix A PSL spheres

A.1 PSL sphere size distributions

In this section the PSL sphere SMPS size distributions are presented.

It can be observed in Figures A1-3 that there are clear nucleation modes in addition to clear but small peaks at around the PSL sphere diameters. It can also be noted that the PSL sphere peaks are unaffected by the thermodenuder.

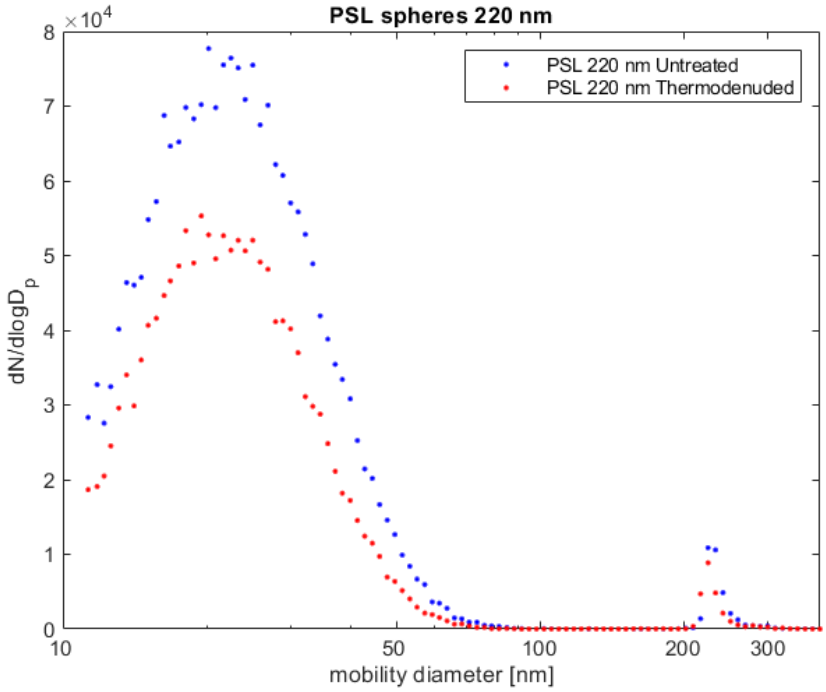

Figure A.1 SMPS size distribution of untreated and thermodenuded 220 nm PSL sphere aerosols.

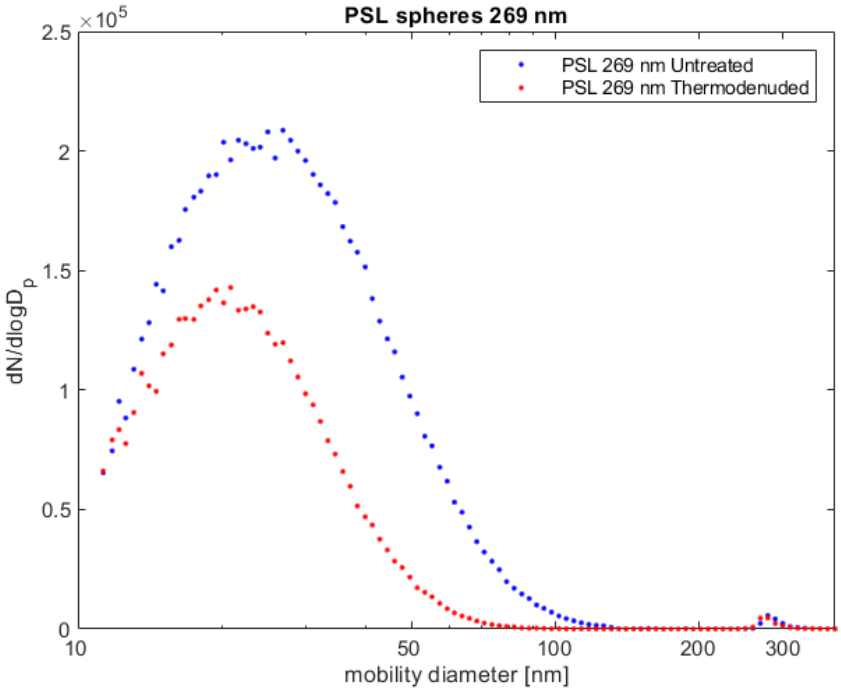

Figure A.2 SMPS size distribution of untreated and thermodenuded 269 nm PSL sphere aerosols.

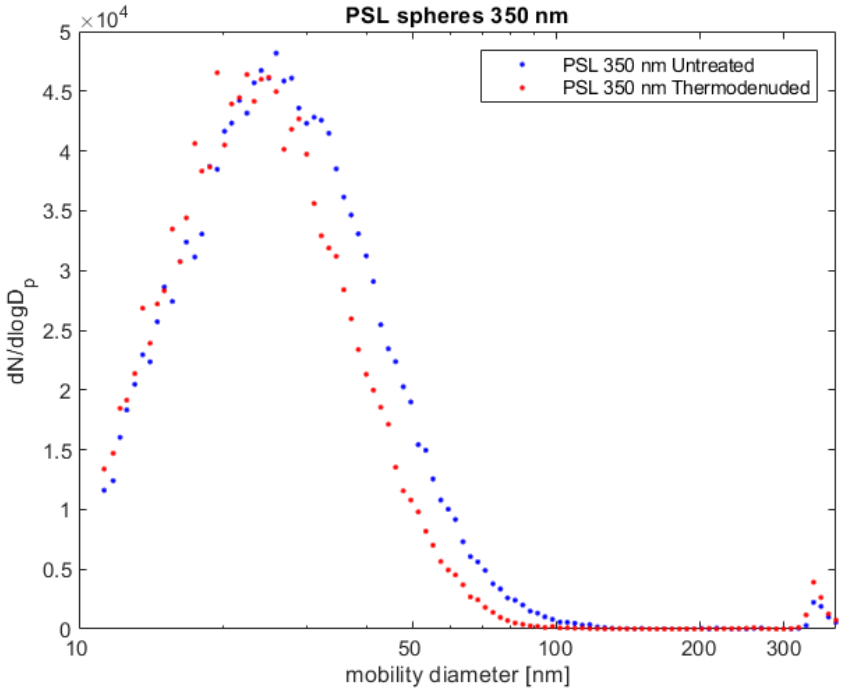

Figure A.3 SMPS size distribution of untreated and thermodenuded 350 nm PSL sphere aerosols.